PB-220 174

NITRIC-OXIDE MEASUREMENT IN A SPARK-IGNITION ENGINE

Robert F. McAlevy, III, et al

Stevens Institute of Technology

Prepared for:

Environmental Protection Agency

January 1973

DISTRIBUTED BY:

NTIS

National Technical Information Service
U. S. DEPARTMENT OF COMMERCE
5285 Port Royal Road, Springfield Va. 22151

APTD-1498

PB 220 174

DEPARTMENT OF MECHANICAL ENGINEERING

NITRIC-OXIDE MEASUREMENT IN A SPARK-IGNITION ENGINE

by

Robert F. McAlevy, III
and
Richard B. Cole

TECHNICAL REPORT ME-RT 73001

for the

Office of Air and Water Programs
Environmental Protection Agency

January 1973

STEVENS INSTITUTE OF TECHNOLOGY
CASTLE POINT STATION
HOBOKEN, NEW JERSEY 07030

Reproduced by
NATIONAL TECHNICAL INFORMATION SERVICE
U.S. Department of Commerce
Springfield VA 22151

68

BIBLIOGRAPHIC DATA SHEET	1. Report No. APTD-1498	2.	3. Recipient's Accession No. PB-220 174
4. Title and Subtitle: Nitric-Oxide Measurement in a Simulated Spark-Ignition Engine			5. Report Date: January 1973 6.
7. Author(s): Robert F. McAlevy, III, Richard B. Cole			8. Performing Organization Rept. No. ME-RT 73001
9. Performing Organization Name and Address: Combustion Laboratory, Department of Mechanical Engineering, Stevens Institute of Technology, Hoboken, New Jersey 07030			10. Project/Task/Work Unit No. 11. Contract/Grant No. * R-801874
12. Sponsoring Organization Name and Address: ENVIRONMENTAL PROTECTION AGENCY, OAWP, Characterization and Control Development Branch, Ann Arbor, Michigan 48105			13. Type of Report & Period Covered 14.

15. Supplementary Notes

*formerly 5R01 AP00847-03

16. Abstracts

To facilitate controlled, reproducible testing for nitric-oxide (NO) generation, a mechanical analog for the spark-ignition was designed, instrumented and tested. The analog provides for constant-volume combustion followed by product-gas expansion through a cam-driven poppet valve, giving pressure-time histories like those of spark-ignition engines. Measurements of NO concentrations in the product gas were made several seconds after combustion both with and without product-gas expansion. NO concentrations were independent of the rate at which product gases were expanded. Ultraviolet absorption by the (0,0) gamma band of NO (2265A) was used to monitor these NO concentrations. Efforts to measure NO concentrations during constant-volume combustion were impeded by unanticipated strong background absorption by CO_2. This rendered the combustion chamber opaque during combustion and precluded monitoring of NO absorption. Absorption measurements at longer-wavelength absorption bands of NO may escape such "masking", but this possibility appears marginal, except for drastically decreased absorption path lengths.

17. Key Words and Document Analysis. 17a. Descriptors

Air pollution
Nitric oxide
Spark ignition engines
Simulation
Combustion
Design
Monitoring
Measurement

17b. Identifiers/Open-Ended Terms

17c. COSATI Field/Group 13B

18. Availability Statement	19. Security Class (This Report)	21. No. of Pages
Unlimited	UNCLASSIFIED	76
	20. Security Class (This Page) UNCLASSIFIED	22. Price $3.00 0.95

FORM NTIS-35 (REV. 3-72)

USCOMM-DC 14952-P72

APTD-1498

NITRIC-OXIDE MEASUREMENT IN A SIMULATED SPARK-IGNITION ENGINE

by

Robert F. McAlevy, III
Richard B. Cole

Combustion Laboratory
Department of Mechanical Engineering
Stevens Institute of Technology
Hoboken, New Jersey 07030

for the

Office of Air and Water Programs
ENVIRONMENTAL PROTECTION AGENCY

Grant No. R-801874
(Formerly 5R01 AP00847-03)

January 1973

ia

EPA Review Notice

This report has been reviewed by EPA and approved for publication. Approval does not signify that the contents necessarily reflect the views and policies of the Environmental Protection Agency, nor does mention of trade names or commercial products constitute endorsement or recommendation for use.

ABSTRACT

To facilitate controlled, reproducible testing for nitric-oxide (NO) generation, a mechanical analog for the spark-ignition was designed, instrumented and tested. The analog provides for constant-volume combustion followed by product-gas expansion through a cam-driven poppet valve, giving pressure-time histories like those of spark-ignition engines.

Measurements of NO concentrations in the product gas were made several seconds after combustion both with and without product-gas expansion. NO concentrations were independent of the rate at which product gases were expanded. Ultraviolet absorption by the (0,0) γ band of NO (2265A) was used to monitor these NO concentrations.

Efforts to measure NO concentrations during constant-volume combustion were impeded by unanticipated strong background absorption by CO_2. This rendered the combustion chamber opaque during combustion and precluded monitoring of NO absorption. Absorption measurements at longer-wavelength absorption bands of NO (e.g., (0,2) γ band at 2580 A) may escape such "masking", but this possibility appears marginal, except for drastically decreased absorption path lengths. Further efforts in this direction were beyond the scope of the present, abbreviated program.

This report was submitted in fulfillment of Grant NO. R-801874 under the sponsorship of the Office of Air and Water Programs, Environmental Protection Agency.

CONTENTS

Section		Page
I	Conclusions	1
II	Recommendations	3
III	Preface	5
IV	Introduction	7
V	Analog Device	9
VI	Nitric-Oxide Monitoring Technique	15
	Post-Combustion Measurements	15
	Measurements During Combustion	22
VII	List of Publications	37
VIII	References	39
IX	Appendix	43
	Program Listing	57

Preceding page blank

FIGURES

		Page
Fig. 1	Automotive Engine Analog	10
Fig. 2	Poppet Value Detail	12
Fig. 3	Comparison of Spark-Ignition-Engine and Analogue-Device Pressure Histories	14
Fig. 4	Steady-State Ultraviolet-Absorption Apparatus	16
Fig. 5	Reference Gas Absorption Scans	17
Fig. 6	Nitric-Oxide-Absorption Calibration Curve	18
Fig. 7	Dependence of Nitric-Oxide Product-Gas Concentration on Initial Pressure	19
Fig. 8	Dependence of Nitric-Oxide Product-Gas Concentration on Equivalence Ratio	20
Fig. 9	Flash-Lamp Circuit	23
Fig. 10	Spectral Distribution of Flash-Lamp Source	26
Fig. 11	Absorption by 4040 ppm-NO (in N_2) Reference Gas (Total Pressure: 240 psig)	27
Fig. 12	Absorption by Products at Various Equivalence Ratios (Φ) and Times Before and After Peak Pressure (P_{max})	28
Fig. 13	Absorption by Products of Stoichiometric Combustion at Peak Pressure	29
Fig. 14	Absorption History During and After Firing of Analog Device	30
Fig. 15	Absorption vs. Pathlength in Products of Constant-Volume Combustion of Stoichiometric Octane Air	35

		Page
Fig. A-1	Flow Chart for Equilibrium Constant-Pressure Combustion Portion of Program	48
Fig. A-2	Flow Chart for Equilibrium Isentropic Compression Portion of Program	49
Fig. A-3	Flow Chart for NO Kinetics Portion of Program	50
Fig. A-4	Partial Sample Output from Program-Equilibrium and Kinetic Results After Burning of 1st Shell	52
Fig. A-5	Partial Sample Output from Program-Equilibrium and Kinetic Results After Burning of 2nd Shell	53
Fig. A-6	Partial Sample Output from Program-Kinetic Results Only, After Burning of 10th (Last) Shell	54
Fig. A-7	Calculated Upper and Lower Limits of NO Concentration	55

TABLES

		Page
Table 1	Estimates of Ultraviolet Absorption at 2265A by NO, CO_2, O_2 in Products of Stoichiometric Constant-Volume Combustion of C_8H_{18} and CH_4	32
Table 2	Program Listing	57

SECTION I

CONCLUSIONS

An approach for study of the mechanism of nitric oxide (NO) production in spark ignition engines was developed during the subject program. It involved the use of an experimental analog to the engine combustion and product gas expansion processes and monitoring of NO concentration during these processes by means of a spectroscopic technique with fine-scale time resolution. The intention was to relate NO generation and destruction to the engine processes in order to estabish a rational basis for reducing its emission.

The simulator was developed, installed and operated successfully. As expected, its operation was more reproducible than that of an actual spark ignition engine, and the range of parameter variation was broader than that of an actual engine. It fills the gap between the more fundamental research laboratory studies of NO kinetics (say, with a shock-tube or well-stirred reactor) and the actual engine. It should play a useful role in this regard.

The development of the time-resolved spectroscopic technique was thwarted by a combustion product of unanticipated strength as a light absorber in the wavelength region of critical interest. At the outset of the program there was no indication in the technical literature that the interfering specie, excited-state CO_2, would play such a powerful role. Following isolation of the origin of the difficulty with the proposed technique, there was insufficient time for its successful resolution prior to termination of the program.

SECTION II

RECOMMENDATIONS

The subject experimental analog of the spark ignition engine should be exploited for the production of data to fill the gap between that from actual engines and that from fundamental research laboratory apparatus, insofar as the NO production and destruction mechanisms are concerned.

The subject NO-monitoring technique should be extended to overcome the problems due to the presence of excited-state CO_2 in the combustion problems.

The published work of others, for example, that of Shahed and Newhall [27] which involves a similar NO-monitoring technique and makes no mention of interference by CO_2, should be critically re-examined.

Preceding page blank

SECTION III

PREFACE

This is a report of an investigation of nitric-oxide (NO) generation in a simulated spark-ignition engine, supported, in part, by Environmental Protection Agency Grant No. R-801874 (formerly PHS Research Grant No. 5R01 AP00847-D3).

The engine simulator design, performance and operating characteristics has been reported in detail (Hodges, J.L., Kurylko, L. and McAlevy, R.F., III, "Nitric Oxide Measurement in a Simulated Spark Ignition Engine", Report No. ME-RT-73008, Stevens Institute of Technology, Hoboken, N.J., January 31, 1971). It forms the framework for, and continuity with, the previously unreported material dealing with computer calculations of NO in the simulator and NO monitoring instrumentation. These activities were limited by the availability of funding.

Preceding page blank

SECTION IV

INTRODUCTION

The automotive spark ignition engine is responsible for a large fraction of the man-made nitric oxide found in the lower atmosphere. Nitric oxide at concentration levels typical of urban environments catalyzes photochemical reactions involving ultraviolet light and unburned hydrocarbons from automotive exhaust gas. The results of these reactions is the production of that conglomerate of chemical compounds generally referred to as photochemical smog [1,2]. Nitric oxide is also toxic and at typical urban levels may be detrimental to nearby plant and animal life.

Early attempts to deduce the thermochemical processes which lead to excessive nitric oxide emission from spark ignition engines involved an analysis of the steady-state exhaust-gas concentration of nitric oxide as a function of such engine operating parameters as compression ratio, fuel-air ratio, engine speed, etc. [3,4,5]. These data, in conjunction with kinetic schemes which evolved from furnace and shock tube experiments [6,7], provided a basis for a kinetic model of the formation and subsequent partial decomposition of nitric oxide during the combustion and expansion of the product gas in spark-ignition engines [8]. Steady-state nitric-oxide measurement techniques have utilized the mass spectrometer [3], spectrophotometer [4], and wet chemistry [5].

There have been relatively few attempts to obtain time-resolved NO-concentration measurements in spark-ignition engines. A periodic sampling device was used to obtain quasi-temporal measurements by Wimmer and McReynolds [8]and later by Starkman [9]. Newhall related the absolute infrared gas emission at the 5.3μ fundamental of nitric oxide to NO-concentration histories in spark-ignition engines [10]. LaVoie, et al., have related NO-concentration histories in spark-ignition engines to the continuous visible radiation resulting from a photochemical reaction involving nitric oxide and atomic oxygen [11]. Their experimental procedure was verified by monitoring several wavelengths in the continuum and by adding nitric oxide to the incoming charge. Extensions of these techniques are described in References 19-21.

Most current theoretical studies of nitric-oxide formation in spark-ignition engines assume that the Zeldovich mechanism [6, 7], or a slight modification thereof (19-22), is applicable. That is to say,

$$N_2 + O \rightleftharpoons NO + N \quad (1)$$

$$N + O_2 \rightleftharpoons NO + O \quad (2)$$

$$N + OH \rightleftharpoons NO + H \quad (3)$$

Preceding page blank

Generally, the oxygen atom is assumed to be in equilibrium with its molecule and nitrogen atoms are assumed in the steady state [11,19-22].

As a consequence of the strong temperature gradients within the combustion chamber during and immediately after combustion, there will also exist strong nitric-oxide-concentration gradients. In a system of this complexity, in situ experimental verification of the theoretical model is essential. The spark ignition engine is, however, a poor vehicle for these studies. Cycle-to-cycle variations in peak cylinder pressure (up to 15 percent standard deviation [12]) can introduce an unacceptable degree of data scatter for any concentration measurements. Many second-order effects, such as spark advance, piston motion during combustion, and fall in volumetric efficiency with rpm, unnecessarily complicate interpretation of experimental results. Additionally, the flexibility of an engine is limited. The possible range of variables, such as peak compression pressure, rate of expansion, and fuel-air ratio is low. For these reasons it was decided to develop an experimental analog device which would simulate, as closely as possible, pertinent phenomena occurring in real engines, while eliminating irrelevant effects and being capable of attaining a degree of precision not possible with actual engines.

The analog device was also instrumented to allow spectroscopic measurements of NO concentrations within the chamber. Ultraviolet absorption by NO at about 2260A was used first to determine NO concentration in post-firing combustion products in the chamber. Based on these results, later spectroscopic efforts were directed toward measuring NO-concentration histories during combustion.

A computer program was developed in order to relate experimental observations from the analog device with a theoretical description of the chemical-kinetics of NO formation. The program was first developed to yield predictions of combustion-chamber pressure and spatial distributions of temperature and equilibrium species concentrations (including NO) (original program, Ref. 23). Finally, modified Zeldovich kinetics for NO formation were superimposed on previous equilibrium calculations so as to allow prediction of local NO concentrations within the chamber. Rather than including a model of flame-front propagation during combustion, the program relates thermodynamic states within the combustion to time by way of input data for the experimentally-observed pressure history in the chamber.

SECTION V

ANALOG DEVICE

Design

In order to design an acceptable alternative, for research purposes, to the spark-ignition engine, it was necessary to define first those disadvantages peculiar to the spark ignition engine and then determine the basis for those disadvantages.

There is considerable evidence that the principal reason for excessive cycle-to-cycle variation in peak engine pressure is the motion of the charge within the combustion chamber prior to ignition [13,14]. That is, the early rate of pressure rise appears a strong function of the local gas velocity, in the vicinity of the spark plug, just before ignition. Turbulence of the incoming charge will result in more intimate mixing and an increase in flame-front area, with an increase in flame velocity and a reduction in susceptibility to detonation. However, pressure traces obtained by igniting a quiescent fuel-air mixture should be considerably more reproducible than those obtained from engines; detonation of quiescent mixtures can be inhibited by reducing flame path length. Additionally, an actual engine is constrained to deliver at least enough useful work to overcome frictional losses. It might be desirable, however, to expand the combustion product gas more slowly than would be possible with an engine. And thus expand the time scale over which the NO kinetics can be observed.

The analog device, then, is essentially a cylindrical, constant-volume bomb (Fig. (1)). A spark plug is mounted in one end of the combustion chamber, along the axis of symmetry, with a cam-driven poppet valve in the other end. After combustion the poppet valve is opened, allowing some of the product gas to exit the chamber. By controlling the rate at which the gas leaves the chamber, it is possible to modulate cell pressure as a function of time. The product gas within the combustion chamber does work to expel part of the gas mixture rather than on a moving piston. The effect is, however, analogous to the expansion of the product gas in an actual engine.

The poppet valve and ignition breaker point cams are mounted on a common shaft which is connected, through a solenoid-operated wrap-spring clutch, to a continuously operating d-c motor. The time interval between ignition and poppet valve opening is controlled by adjusting the relative angular position of the two cams. Valve lift was determined as a function of the rate of change of gas pressure with time by coupling the equations for choked flow and isentropic expansion, and the perfect gas law. That is, assuming choked flow at the poppet valve throat,

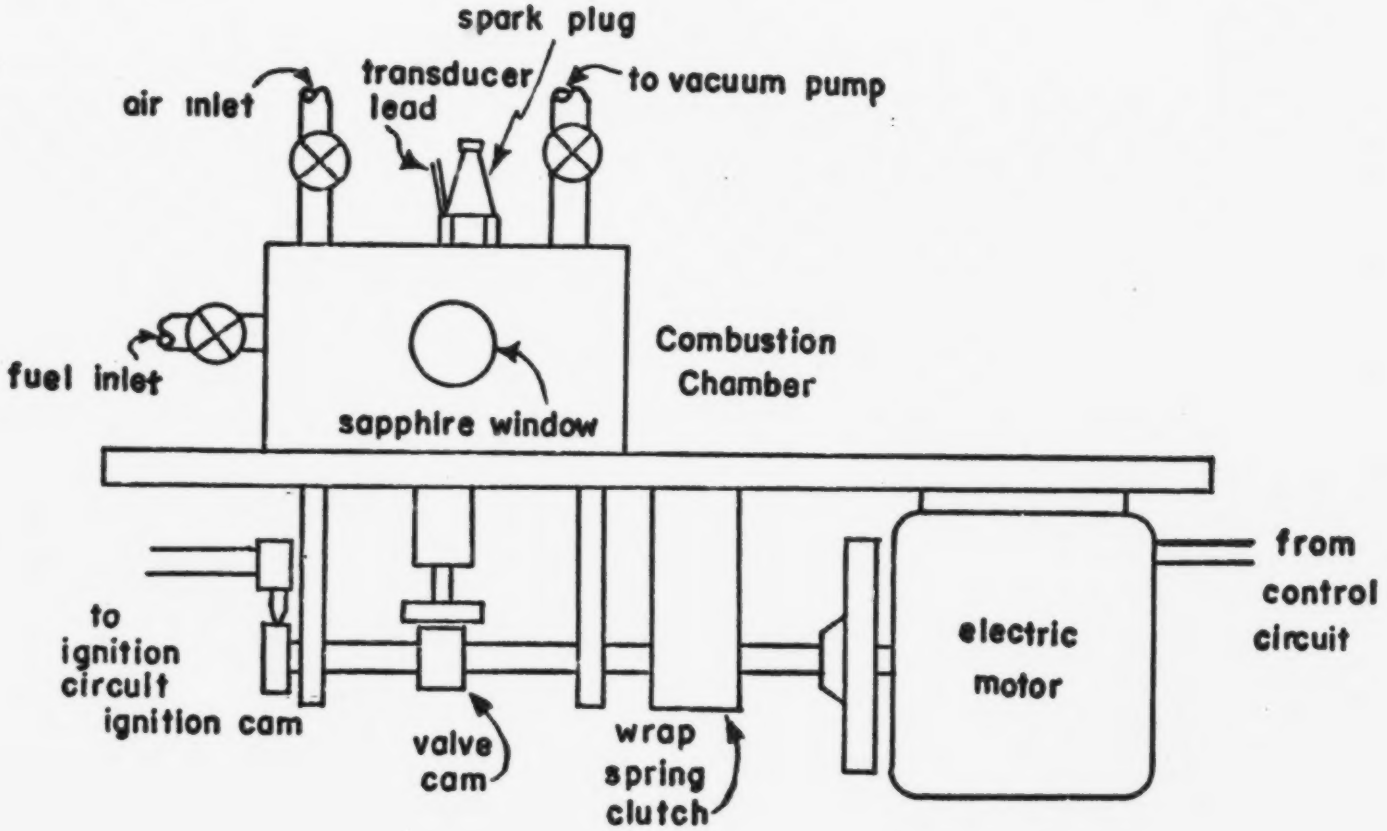

Figure 1 Automotive Engine Analog

$$w/A = \left(kg/R \left(\frac{2}{k+1} \right)^{\frac{k+1}{k-1}} \right)^{1/2} P_0/T_0{}^{1/2} \qquad (4)$$

$$T_0/T_0' = (P_0/P_0')^{(k-1)/k} \quad . \qquad (5)$$

$$P_0V_0 = mRT_0 \qquad (6)$$

then

$$m = \left(V_0/R \frac{P_0'^{(k-1)/k}}{T_0'} \right) P_0{}^{1/k} \qquad (7)$$

and

$$dm/dt = \left(\frac{V_0}{Rk} \frac{P_0'^{(k-1)/k}}{T_0'} \right) (P_0{}^{(1-k)/k}) dP_0/dt \qquad (8)$$

combining equations (4) and (8)

$$A \left(kg/R \left(\frac{2}{k+1} \right)^{\frac{k+1}{k-1}} \right)^{1/2} P_0/T_0{}^{1/2} = \left(\frac{V_0}{Rk} \frac{P_0'^{(k-1)/k}}{T_0'} \right) \times (P_0{}^{(1-k)/k}) dP_0/dt \qquad (9)$$

eliminating T_0 and solving for A,

$$A = \frac{V_0}{k\sqrt{kRgT_0'}} \left(\frac{2}{k+1} \right)^{(k+1)/2(k-1)} \frac{d(P_0/P_0')/dt}{(P_0/P_0')^{(3k-1)/2k}} \qquad (10)$$

The required flow area is determined from equation (10). This is matched by the valve lift area, which is the surface area of the conical frustum of slant height, t (see Fig. 2). The valve lift area is related to the valve stem lift by

$$A = \pi s \sin \alpha (d - \sin \alpha \cos \alpha)(1 + \cos^2 \alpha)^{1/2} \qquad (11)$$

Combining equations (10) and (11):

$$s(d - s \sin \alpha \cos \alpha) = \frac{V_0 (d(P_0/P_0')/dt)/(P_0/P_0')^{(3k-1)/2k}}{\pi \sin \alpha (1 + \cos^2 \alpha)^{1/2} (k) \sqrt{kRgT_0'} (2/(k+1))^{(k+1)/2(k-1)}}$$

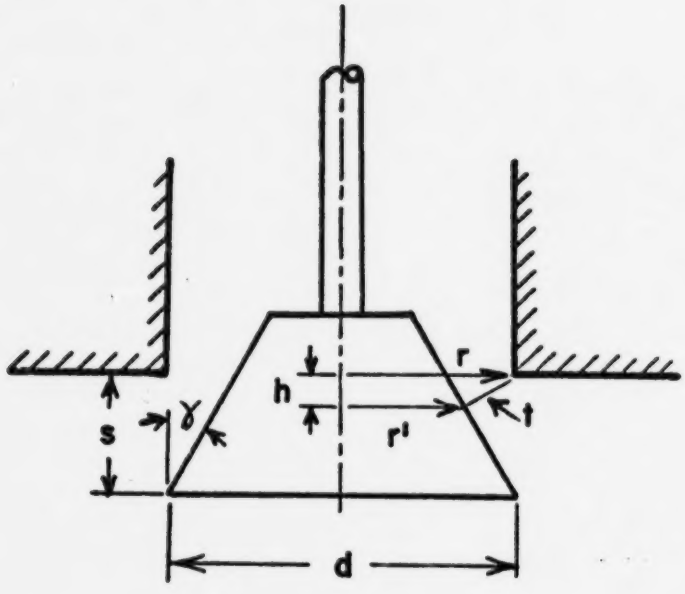

Figure 2 Poppet Valve Detail

A computer program was developed to generate the required cam profile for the valve lift requirements since conventional graphical techniques were not sufficiently accurate.

Operation

To initiate a test cycle, a microsyringe was used to introduce fuel to the evacuated combustion chamber. The chamber, which was maintained at a constant temperature, was then pressurized with dry air. In this manner conditions were produced which corresponded to those in an engine just prior to ignition. Engagement of the clutch resulted in precisely one revolution of the cam shaft. As the shaft rotated, the ignition breaker points closed, igniting the fuel-air mixture.

Performance

A comparison of typical pressure histories obtained with the analog device and an actual CFR spark ignition engine is presented in Fig. (3). The analog device pressure traces are considerably more reproducible than the engine pressure traces. The rates at which pressure rises and falls during combustion and expansion are slightly less with the analog device than with the engine. This could have an influence on the kinetics of nitric oxide formation and decomposition during combustion [22]. The lower rate of pressure rise in the analog device is a consequence of the low flame speed typical of quiescent gas mixtures. The maximum rate of expansion is limited by the mechanical design of the apparatus, the practical limit being imposed by maximum inertial forces in the valve-cam system.

Pressure traces were obtained at initial pressures between 25 and 125 psia, and initial temperatures between 250 and 450 deg. F. Most data were obtained with the initial temperature of 350 deg. F. Peak measured pressures varied between approximately 125 and 650 psia. In the analog the volumetric efficiency was 100 percent and the combustion proceeded at constant volume. This resulted in peak pressures generally higher than those encountered in an engine where residual gas causes dilution of the active charge and where piston ring blow-by would offset maximum pressures.

Iso-octane fuel was used in all runs.

No detonation was observed in any of the tests.

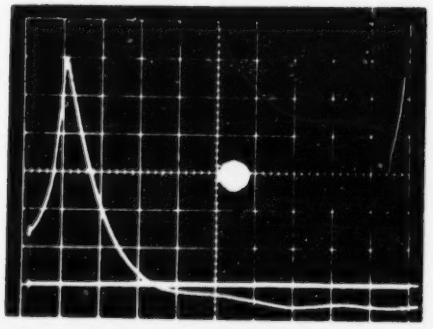

8:1 COMPRESSION RATIO
980 RPM
100 psi/div
5 ms/div

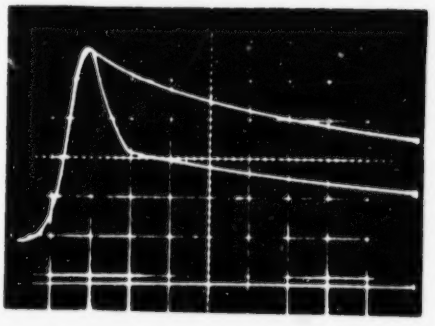

INITIAL TEMPERATURE: 350°F
INITIAL PRESSURE: 125 psia
EQUIVALENCE RATIO: 1.1

100 psi/div
20 ms/div

Note: Analog device pressure traces represent superposition of constant volume and expansion runs

Figure 3 Comparison of Spark-Ignition-Engine and Analog-Device Pressure Histories

SECTION VI

NITRIC-OXIDE MONITORING TECHNIQUE

Post-Combustion Measurements

A new monitoring technique was developed to measure nitric oxide product gas concentration a few seconds after combustion. The technique was used in place of established methods because it was hoped that it could be eventually extended to obtain time-resolved in situ measurements during combustion.

Nitric-oxide concentration in the product gas was related to the absorption of ultraviolet light at the $(0,0)\gamma$ band of nitric oxide between 2260 A and 2270 A [15]. A schematic of the monitoring apparatus is presented in Fig. (4). It was found that, at a fixed temperature, the absorbance of the gas mixture was a function only of the partial pressure of nitric oxide. At low NO partial pressures the measured absorption coefficient agreed with published values [16].

Absolute or integrated band intensities were calculated and compared with published data [17]. Use of a single beam monochromator made acquisition of absolute intensities difficult and imprecise. Allowing for this, the data correlated reasonably well with the literature.

As an experimental control, calibration curves were obtained, using a reference gas (a mixture of 4040 PPM NO, balance N_2), prior to and after each series of experimental runs. Reference gas absorption traces are presented in Fig. (5). The calibration curves consisted of plots of the reference gas absorbance between and at each of the two band heads versus the known nitric oxide partial pressure (Fig. (6)). Subsequently, the absorbance of the combustion product gas at the two band heads was measured, and, using the calibration curves, the corresponding partial pressure of nitric oxide was determined. Measurements of the total pressure of the product gas following combustion permitted the calculation of the nitric oxide concentration in the exhaust gas as a function of such parameters as initial pressure, initial temperature, equivalence ratio and rate of expansion.

Discussion

As expected, NO concentration was a weak function of initial temperature and pressure (Fig. (7)), and a strong function of equivalence ratio (Fig. (8)). Evident is the "inverted U" characteristic of measurements made on actual spark ignition engines [3,4,8]. Measured NO concentrations were somewhat higher than would be expected in engines. There are numerous possible explanations for this. First, the residual exhaust gas fraction carried over from one cycle to the next will tend to dilute the incoming charge, with a consequent reduction in

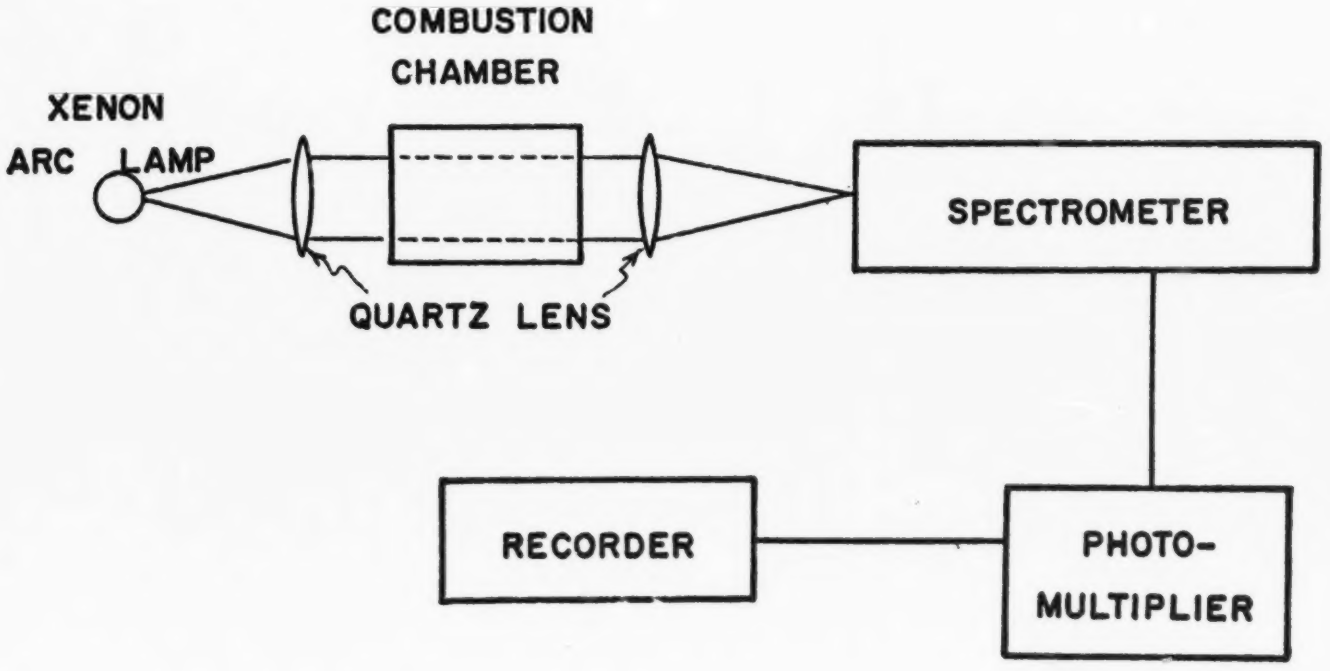

Figure 4 Steady-State Ultraviolet-Absorption Apparatus

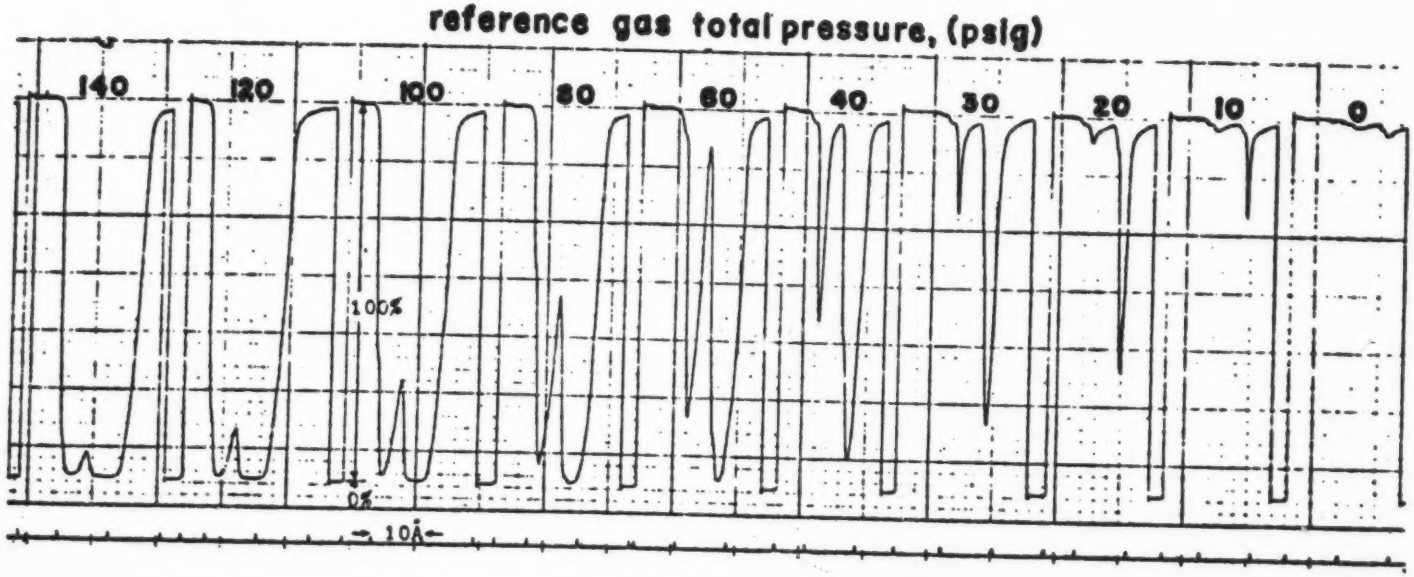

Figure 5 Reference-Gas-Absorption Scans

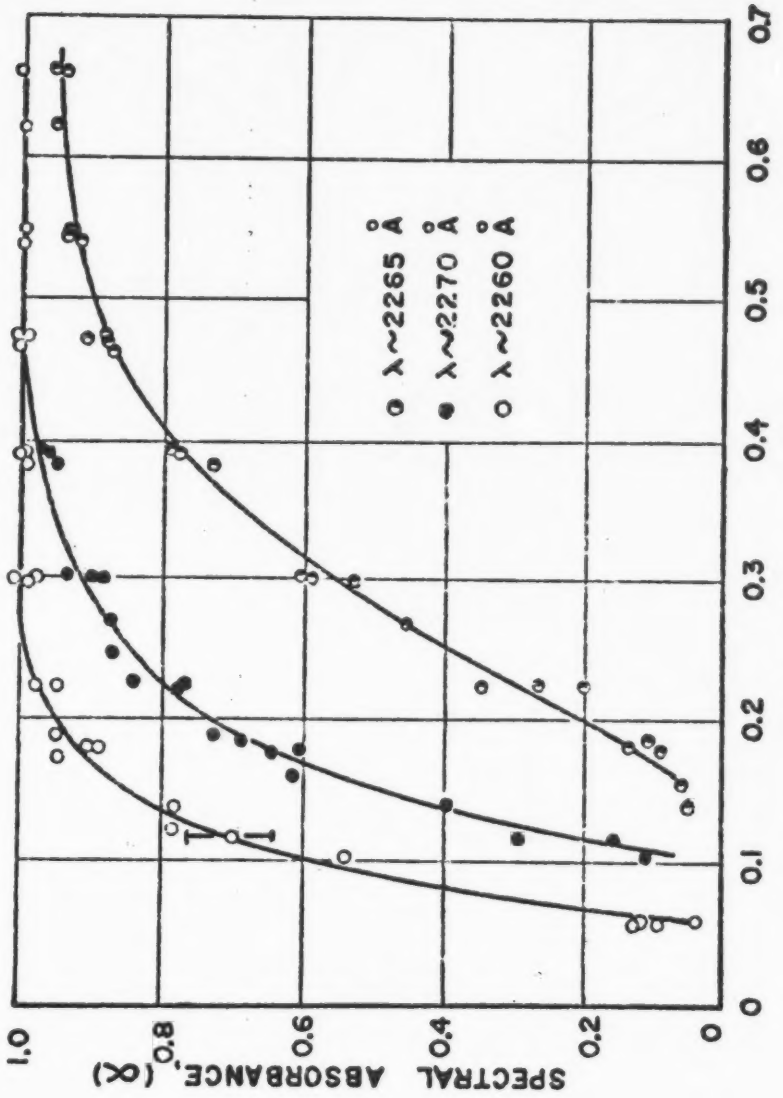

Figure 6 Nitric-Oxide-Absorption Calibration Curve

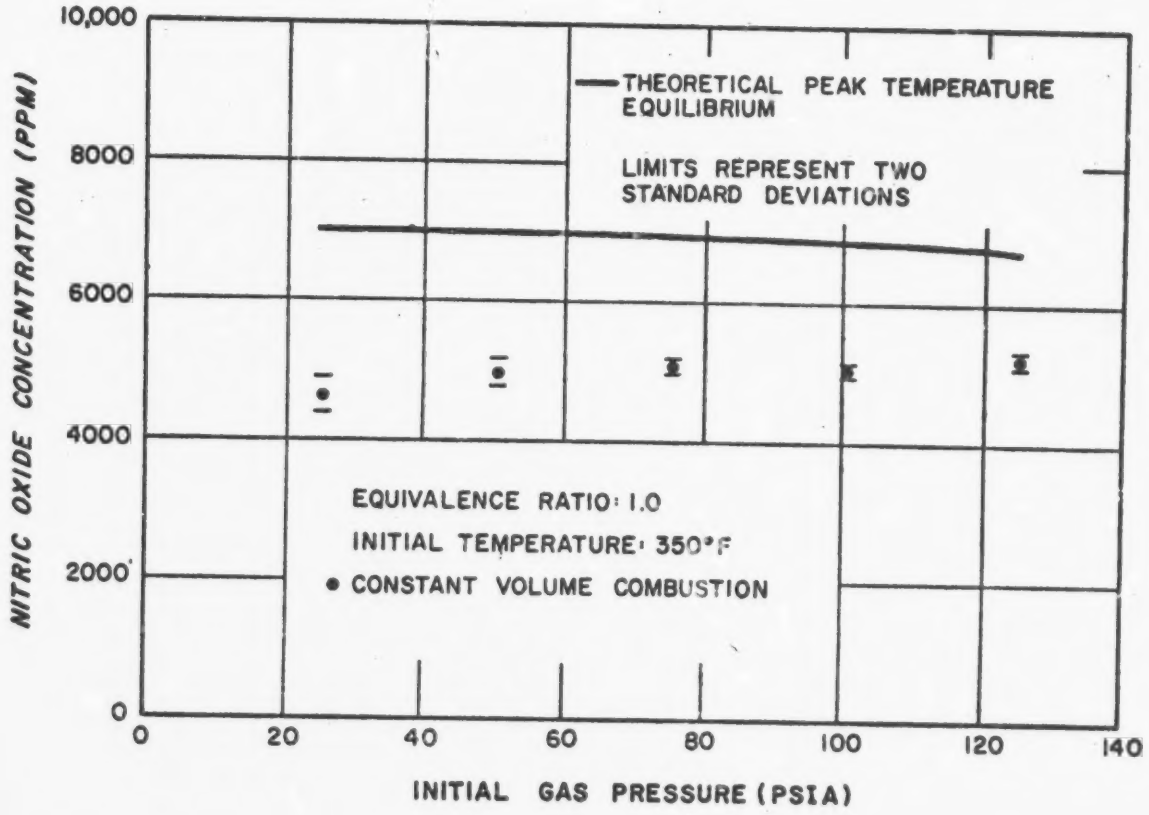

Figure 7 Dependence of Nitric-Oxide Product-Gas Concentration on Initial Pressure

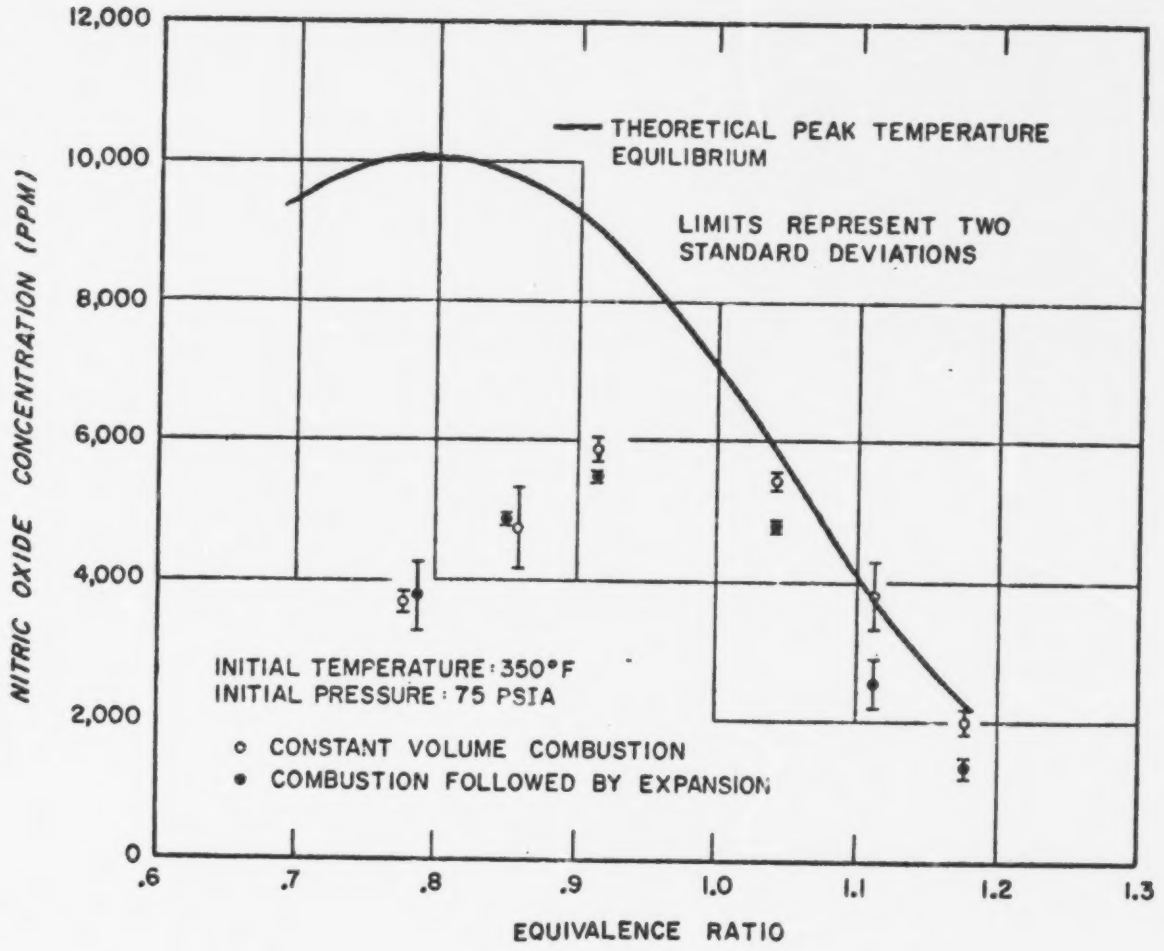

Figure 8 Dependence of Nitric-Oxide Product-Gas Concentration on Equivalence Ratio

peak cycle temperature (this effect is consciously used to reduce nitric oxide emissions from engines in the familiar exhaust gas recycle technique). In the analog device, the residual exhaust fraction is virtually zero. The presence of moisture in the air similarly suppresses peak cycle temperatures [18]. Dry air was used in all experimental runs described herein. Additionally, in engines piston ring blow-by and piston motion allow the gas to expand during combustion, again tending to reduce peak cycle temperature. These effects are also absent in the analog device, and so, as a consequence of the increase in peak cycle temperature, higher measured nitric oxide concentrations would be expected.

A particularly interesting effect was noted when measured nitric oxide concentrations obtained when the product gas was expanded as rapidly as possible following combustion were compared with nitric oxide concentrations in the product gas after constant volume combustion. The measured nitric oxide concentrations were virtually the same in each case. This would tend to imply that piston motion plays a relatively minor role in the events which lead to the freezing of nitric oxide in spark ignition engines.

Current kinetic schemes invariably assume that the only means by which a reduction in product gas temperature can be obtained is the isentropic expansion of that gas (i.e., through piston motion). Effects such as heat transfer to the wall, radiation, etc. are thought, quite correctly, to have only a minor influence on the bulk temperature of the gas. However, it should be noted that strong temperature gradients (up to 400 deg F) exist across the combustion chamber. Nitric oxide equilibrium concentration in the hottest part of the product gas is about six times that in the coolest part [11]. That portion of the gas mixture richest in NO is closest to the wall, where wall cooling effects would be expected to have the greatest influence. Additionally, any mixing of the hot and cool segments of the product gas could also result in freezing of the nitric oxide. Apparently the "rate of expansion", or more specifically, the rate at which gas pressure changes with time, is reflective only of the rate at which the average, or bulk, temperature changes with time. Local cooling rates, however, would be expected to exceed the average value in precisely that portion of the mixture richest in nitric oxide.

Measurements During Combustion

The approach described above and in Ref. 23 was adapted to measuring NO concentrations in situ during combustion. This direction was indicated by the results of post-combustion NO measurements [23]. These included the observation that NO "freezing" in product gas did not appear to depend strongly on piston motion but rather on processes occurring during combustion.

Preliminary spectrographic data were taken during combustion by replacing the steady arc-lamp and the photomultiplier used in post-combustion measurements (see Fig. 4) with a Xenon flash-tube and spectrographic film, respectively. The experiments involved obtaining a spectrograph by repeated exposures to the flash-lamp source. In order to achieve suitably high densities on the spectrographic film, the light source was fired (repetitively) at selective times either during or after combustion for a succession of replicate firings of the analog device. These preliminary measurements, reported in detail in Ref. 23, were not sensitive enough to discern NO prior to 5 msec before the attainment of peak chamber pressure (i.e., 5 msec before the completion of combustion).

Apparatus

To adopt the previously used equipment to NO measurement during combustion, substantial improvements in auxiliary equipment (exhaust hoods, etc.) and in mounting and positioning equipment (for optics, analog device, etc.) were made. These design changes were dictated by both safety and optical alignment considerations, given the decision to continue usage of the analog device and spectrometric instrumentation over an extended time period. The major apparatus development required, however, was of the instrumentation for time-resolved NO measurements during combustion.

The spectrometric instrumentation developed included a new flash-lamp source, modification of the associated trigger circuit, and a new detection system. These new developments were dictated by the desire for a higher sensitivity system which did not require multiple firings of the analog device for each data point; the multiple firings required in preliminary spectrographic measurements (see above) were judged to be impractical.

The flash-lamp source which was developed for time-resolved NO measurements is shown schematically in Fig. 9. The power source for charging the capacitor was an Ascorlight Model 62-509 high-voltage power supply which usually was operated at about 1000 vdc yielding flash energy inputs of about 450 watt-seconds. Linear-pulsed xenon flash tubes (EG & G Models FX42C-3 and FX38A-3) provided a 3" arc of roughly 1000

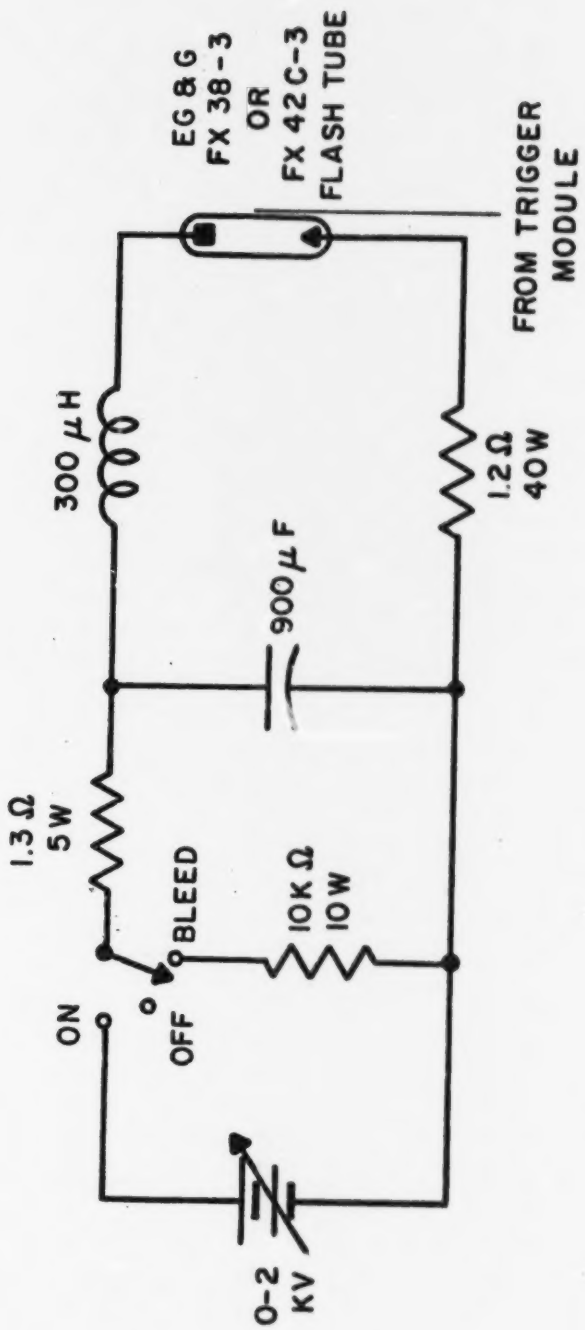

Figure 9 Flash-Lamp Circuit

horizontal-candlepower seconds. The arc was focussed on the spectrometer entrance slit following collimation by a quartz lens and transmission through the sapphire windows of the analog device. The optics, flash-triggering, and time-delay circuit were essentially those detailed in Ref. 23 excepting minor modification of the time-delay circuit. Alignment of the optical system was facilitated by a back light, a 12 vdc, coiled tungsten filament lamp built into the flash-tube mounting. This allowed imaging of the flash tube on the entrance slit of the spectrometer during alignment. The flashes used during NO measurement were of approximately 0.5 msec duration (between 50%-intensity points) and were of ample energy to be detected by the spectrometer detector.

The previously used spectrometer (Jarrell-Ash Model 82-020, 0.5 meter, Ebert type) was equipped with a grating of 1200 lines/mm (3000A blaze) and entrance and exit slits of 50 μn, yielding a spectral slit width of about 1.5A(Ref. 23, p. 118). The f-number of the spectrometer (f/8.6), rather than the associated optics, limited transmission. Tests indicated a hysteresis(backlash) of approximately 1A in the wavelength setting of the monochromator.

The previously used photomultiplier detector [23] was found to be excessively noisy presumably owing to age and usage. A new photomultiplier (EMI Model 9558Q) with fused-silica window, a new photomultiplier housing (EMI Model E258) and a potted dynode chain (EMI Model D113 FL) were adapted to the spectrometer exit aperture. The photomultiplier was powered by a Brandenburg Model 500 power supply, typically operating at 800 to 900 vdc. Photomultiplier output was recorded photographically using an oscilloscope (Tektronix Model 564, with Type 3A3 Dual-Trace Differential Amplifier and Type 2B67 Time Base). Linearity of response of the detection system was verified using calibrated neutral-density filters (quartz substrate).

Discussion

Preliminary testing with the new instrumentation and procedures for time-resolved NO measurements revealed several problems with reproducibility of flash-lamp-source peak intensity and triggering. These problems were sidestepped temporarily with the aim of proceeding as quickly as practical to further evaluation of the proposed approach to NO measurement. Reproducibility of flash-lamp intensity and triggering, while not completely satisfactory, were viewed as good enough to allow rough measurements of NO concentrations during firing of the analog device.

Figure 10 shows the results of successive flash-lamp firings with the test chamber of the analog device evacuated. The spectral distribution and scatter shown are representative of the flash-lamp system used in further testing. While reproducibility is not totally satisfactory, the flatness of the spectral distribution of the lamp radiation is helpful.

Figure 11 shows the spectral distribution of photomultiplier output when the combustion chamber of the analog device was pressurized to 40 psig with a reference gas of 4040 p.p.m. NO - balance N_2. Absorption of radiation from the flash lamp by the two-headed (0,0) γ band of NO centered at about 2265A is evident.

Despite some shortcomings in reproducibility of flash-lamp firing, a series of test firings of the analogue device was made to allow better evaluation of the potential of the time-resolved ultraviolet-absorption approach for measuring NO concentration.

Test firings of the analog device were made at various equivalence ratios, pre-firing pressure and temperature of 4.4 atm and 450^{o}K. Measurements of ultraviolet absorption by the products of combustion were made at various times during combustion (before attainment of peak pressure) and after. In each case comparable measurements were made of photomultiplier output with the test chamber evacuated.

Figures 12 and 13 show the results of spectral-absorption measurements at various times and equivalence ratios. Noteworthy is the apparently high absorptivity of the combustion products over a wide spectral range. This had not been observed in earlier measurements on products well after completion of combustion when the products are cooler and at lower pressure due to heat loss (Ref. 23, also Fig.14). Some effect of this type had been expected owing to the presence of 0_2. However, it was expected that this absorption would not substantially exceed that of NO and that, outside the (0,0) γ band of NO the absorptivity of the products would not exceed approximately 50% [23].

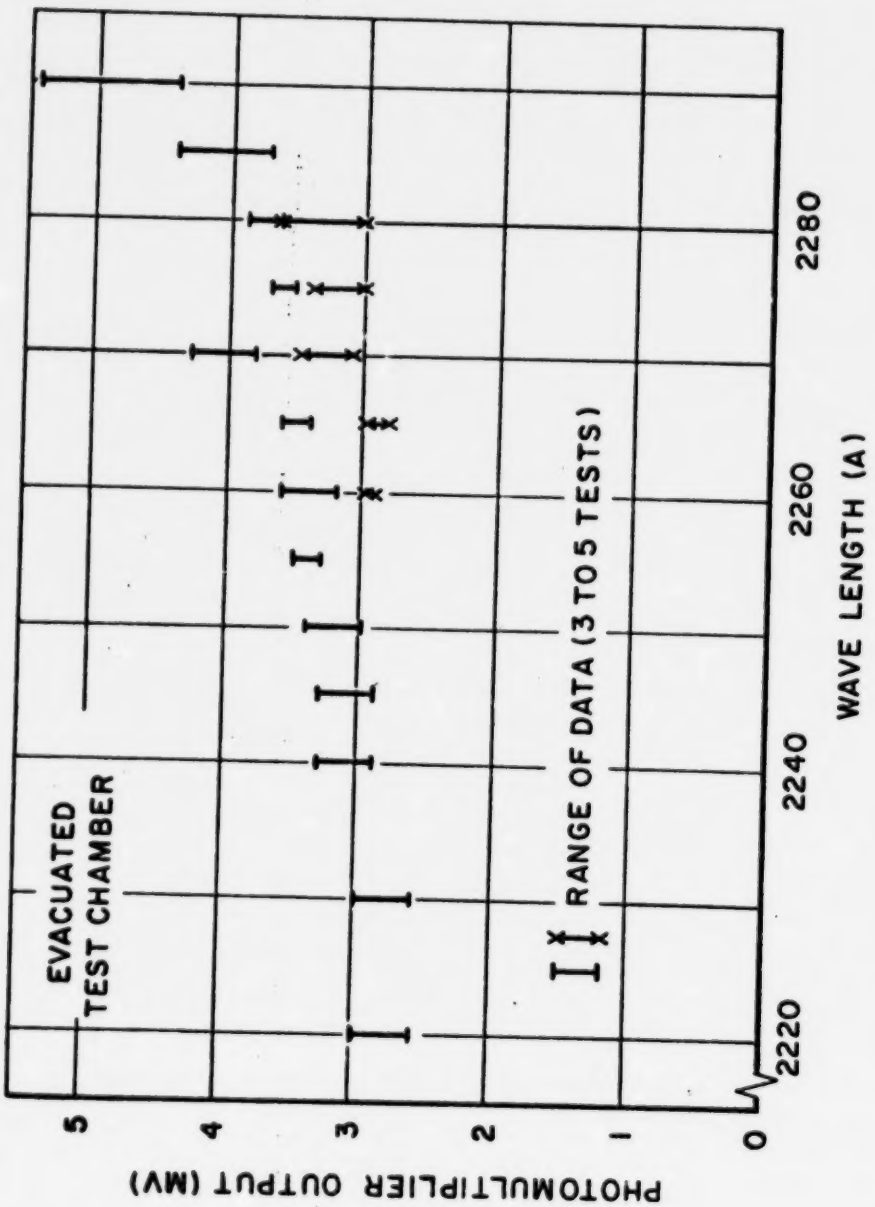

Figure 10 Spectral Distribution of Flash-Lamp Source

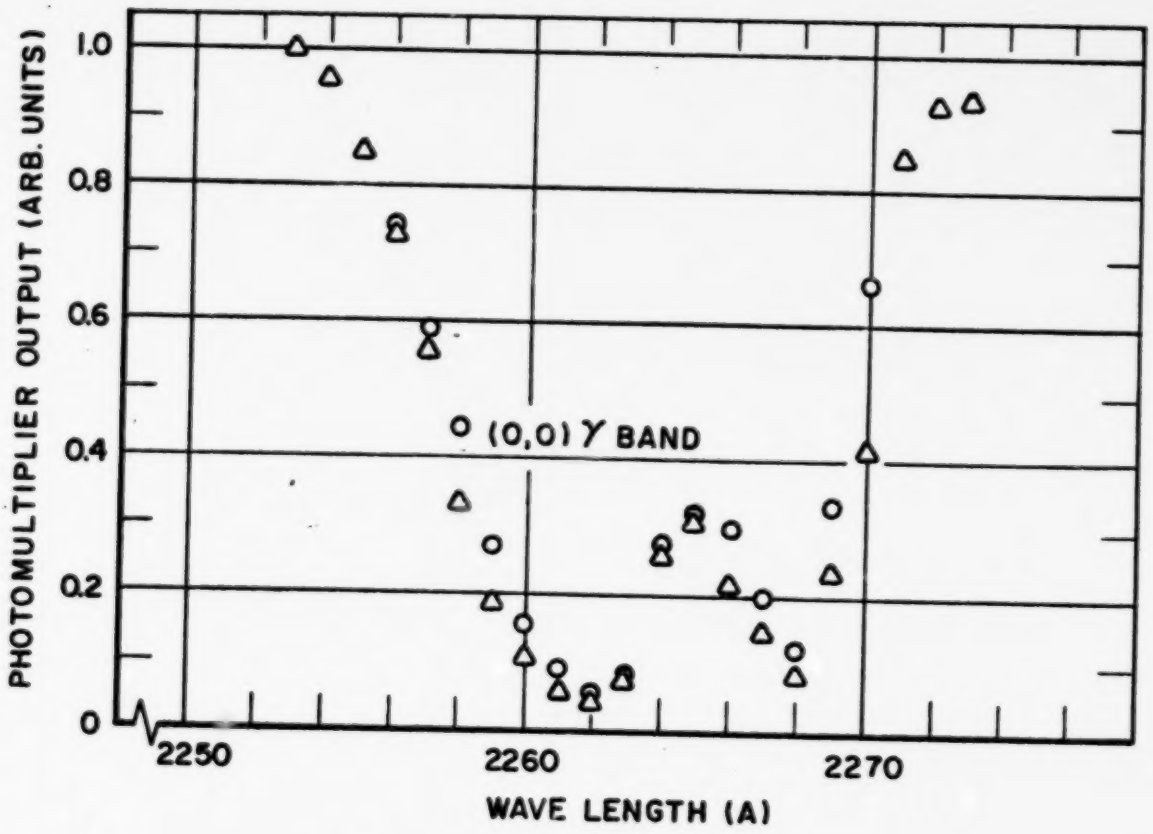

Figure 11 Absorption by 4040 ppm-NO (in N_2)
Reference Gas - Total Pressure: 40 psig

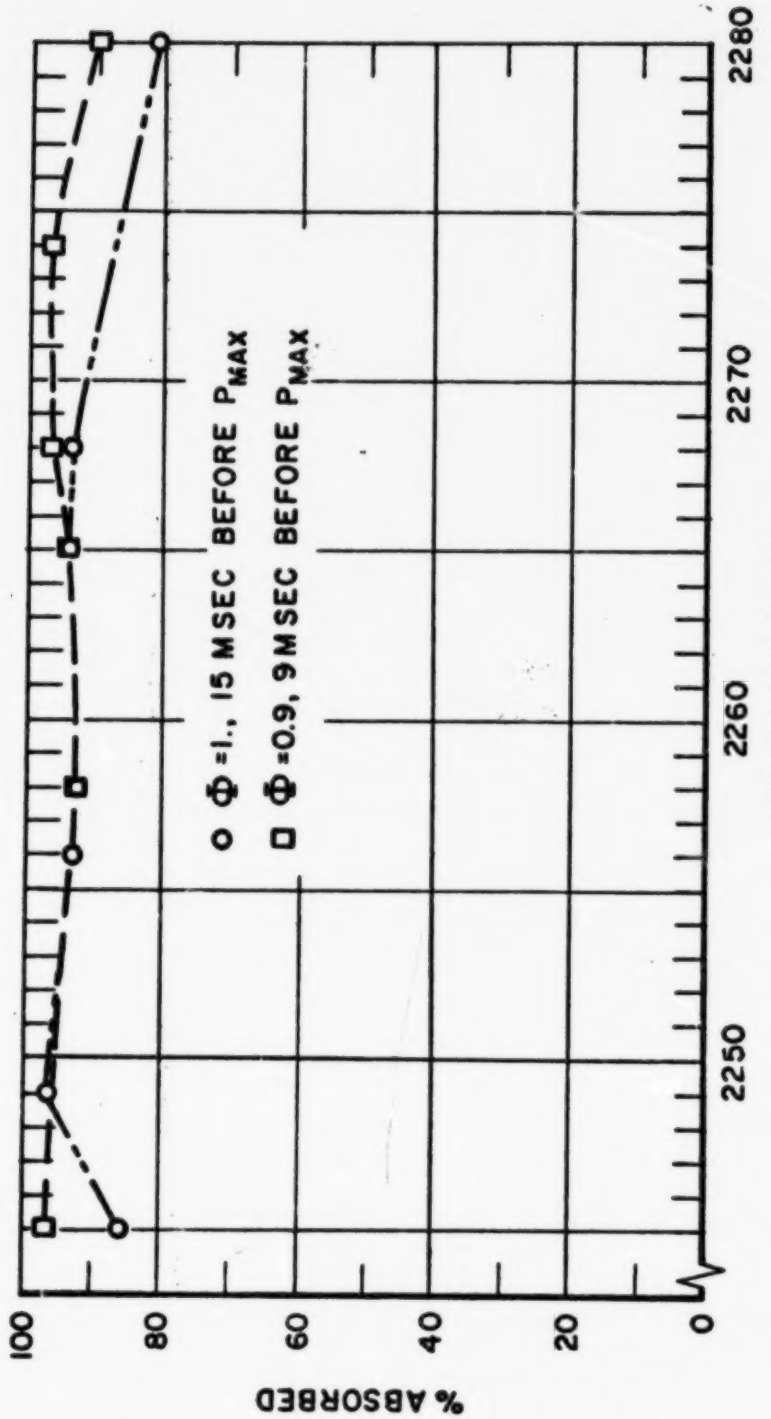

Figure 12 Absorption by Products at Various Equi'alence Ratios (Φ) and Times Before and After Peak Pressure (P_{MAX})

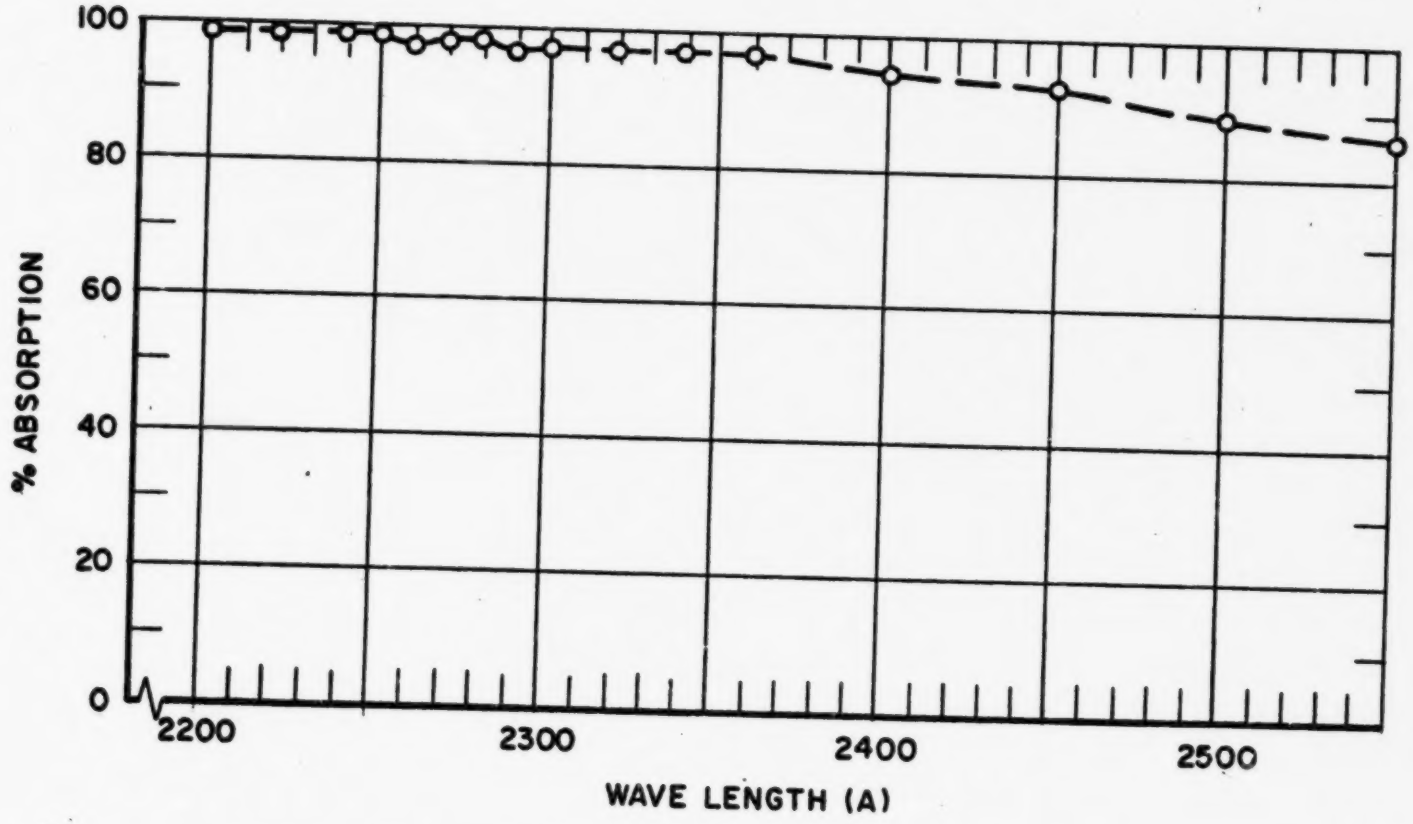

Figure 13 Absorption by Products of Stoichiometric Combustion at Peak Pressure

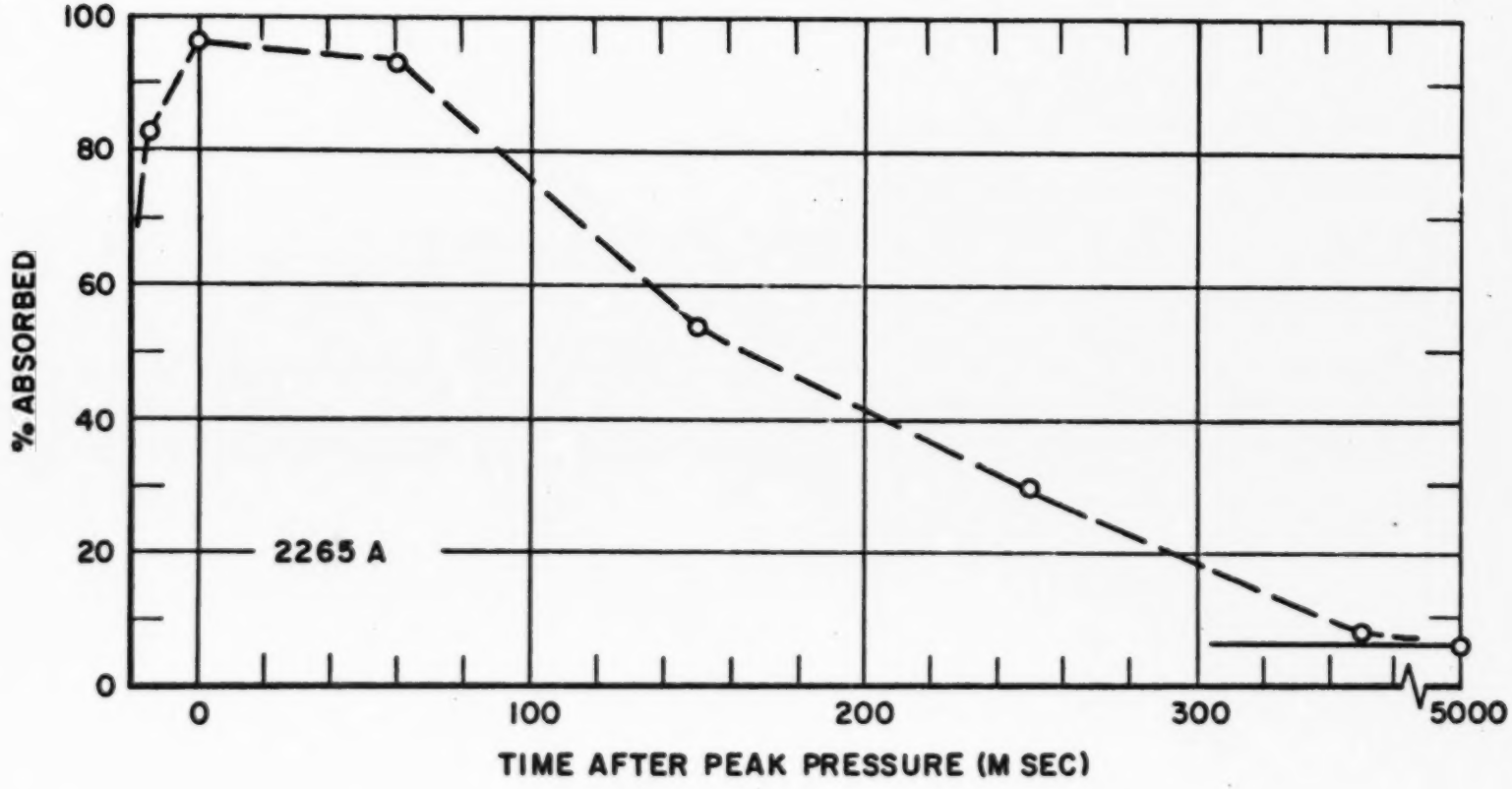

Figure 14 Absorption History During and After Firing of Analog Device

Since the concentration of O_2 in combustion products is strongly dependent on equivalence ratio, absorption due to the Schumann-Runge bands of O_2 should decrease appreciably as the equivalence ratio is increased toward richer combustible mixtures. Tests of rich mixtures in the analog device did not, however, evidence substantial decreases in ultraviolet absorption outside of the (0,0) γ band of NO. Hence, it appeared that either or both of two effects were probably responsible for the broad-band ultraviolet absorption observed in test firings: (i) disruption of the beam through the test section, perhaps due to refraction by flame-front-generated turbulence, or (ii) presence of an unknown broad-band absorbing species.

The possibility of massive disruption of the spectrometric light beam by refractive effects was tested by passing the narrow beam of a CW helium-neon laser through the test cell and onto a small photodetector (ca. 2 mm diameter). The photodetector output was recorded during a test firing, and no major change in signal level was observed. This indicated that beam displacement after passage of the flame front was negligible and not a likely cause of the observed broad-band decreases in photomultiplier output during NO-measurement tests.

A search for possible broad-band absorbers other than O_2 ensued. Carbon-or hydrogen-containing species were focussed on owing to the previously mentioned fact that the observed broad-band ultraviolet absorption was found to be relatively independent of equivalence ratio. Standard references on absorbing/emitting species in flames proved fruitless. Finally, late in the second year of this program, a little-recognized broad-band ultraviolet absorber was identified: CO_2.

Broad-Band Interference (Ultraviolet Absorption) by CO_2

Recent shock-tube studies of the chemical kinetics of NO formation [24] uncovered the fact that the CO_2 molecule exhibits broad-band ultraviolet absorption at elevated temperatures [25]. Apparently this absorption has not been widely cited in the combustion literature because of the paucity of spectrometric combustion studies at the short ultraviolet wavelengths of concern in the present investigation.

Based on the available data for the ultraviolet absorption of CO_2, estimates were made of the ultraviolet (2265A) absorptivity of the products of constant-volume combustion of stoichiometric octane-air mixtures. The optical path lengths considered were those corresponding to the analog device (physical path length: 8.25 cm.). Similar calculations were made for a fuel of lower C/H ratio, CH_4. The results are shown in Table 1.

The results in Table 1 show that the high absorption coefficient of the (0,0) γ band of NO, as measured earlier in the present study [23], render the combustion products in the analog

Fuel (with air)	Species	k, Absorption Coefficient (cm^{-1})	x, Mole Fraction (-)	ℓ', Optical PathLength (cm)	α, Absorption (%)
C_8H_{18}	NO	30 (a) 7 (b)	.022 "	0.60 "	99+ 92
"	CO_2	4.0 (c)	.072	1.95	99+
"	O_2	1.2 (d)	.022	0.60	51
CH_4	NO	30 (a) 7 (b)	.018 "	.45 "	99+ 85
"	CO_2	4.0 (c)	.057	1.43	99+
"	O_2	1.2 (d)	.018	46	42

Notes: (a) Ref. 23

(b) Ref. 16 $\alpha = 1 - \exp\left(- k \ell' x \frac{N_o}{N}\right)$

(c) Ref. 25 $\ell' = \frac{P}{P_{std}} \frac{T}{T_{std}} x (8.25 \text{ cm})$

(d) Ref.23 $\frac{N_o}{N} = 0.61$ (depopulation of ground state of NO)

TABLE 1 Estimates of Ultraviolet Absorption at 2265A by Individual Species in Products of Stoichiometric Constant-Volume Combustion of C_8H_{18} and CH_4

device optically thick for narrow spectral slit widths centered in the (0,0) γ band. However, in the absence of major "background" absorption by CO_2 or O_2, this does not render NO concentration measurements unfeasible. As was demonstrated earlier in the present program (Ref. 23, p. 76) large spectral slit widths, exceeding the NO-band width, render the test gas transparent enough to allow absorption measurements and, hence, NO-concentration measurements.

Unfortunately, however, the results of Table 1 show very high absorption by CO_2 as a "background" absorber. This absorption is over a much broader spectral range than that of the NO band (Ref. 25, also Figure 12). Thus, in contrast with NO absorption, CO_2 absorption is not substantially decreased by increasing the spectral slit width for absorption measurements, i.e., CO_2 absorption, being less spectrally localized than NO, renders the test gas opaque even for large spectral slit widths centered at the (0,0) γ band of NO. This apparently precludes absorption spectrometry in CO_2-containing product gas in the neighborhood of 2265A.

Only two alternatives are apparently possible to escape the obstacle of CO_2 absorption: (i) moving to a different NO absorption band where CO_2 absorption is much lower, rendering the products optically thin, or (ii) decreasing the physical (and, therefore, optical) path length in the analog device.

Relative to the possibility of NO absorption spectrometry at higher wavelengths, it is noteworthy that CO_2 absorption apparently extends little diminished (see Fig. 13) to 2500 to 2600A. Calculations like those for Table I were made using the absorption coefficients of Bowman and Seery [24] at 2358A for CO_2. The results showed only slight improvement (α_{CO_2}=0.98) at this wavelength, corresponding with the (0,1) γ band of NO. The wavelength of the (0,2) γ (2580A) may show some further decrease in CO_2 absorption but probably only marginally so considering the slow decrease in the absorption coefficient of CO_2 with increasing wavelength [25]. Above this wavelength other interfering species, e.g., OH and CO [26] begin to be influential so that little, if any, "window" exists, i.e., combustion products (other than NO) in the analog device are likely to be optically thick and absorption spectrometry is not practical. Detailed consideration of the spectrometric potential of the (0,2) or higher wavelength γ bands for NO concentration measurement might show marginal value, but further investigation, experimentally or theoretically, was precluded by truncation of the present investigation.

The possibility of decreasing the optical thickness (path length) in combustion products of the analog device is also not promising as a route for minimizing interference by the strongly absorbing CO_2 molecule. The physical path lengths required to

allow transmission of a substantial fraction of the spectrometric beam are too short to be practical for a device intended to analogous to a spark-ignition combustion chamber; physical path lengths on the order of less than 2 cm. would be required (Fig. 15).

In summary, then,it appears based on both theoretical and experimental data that ultraviolet absorption by CO_2 precludes spectrometric measurement using the γ bands of NO to determine NO concentrations in high-temperature combustion products of hydrocarbon fuels burned in practical-sized combustion chambers. This conclusion contradicts the basis for the measurements reported by Newhall and Shahed [27] but appears to be firmly grounded. The failure of these earlier workers to observe or consider CO_2 absorption is currently unexplained. The above conclusion, however, does not preclude the possibility of spectrometric NO measurements using the γ bands of NO for non-hydrocarbon (e.g., H_2) combustion systems. Of course, optically-thin configurations with dilute, non-combustible mixtures such as those of the shock-tube investigations of Bowman and Seery [24] are also practical applications of ultraviolet, spectrometric NO detection and measurement.

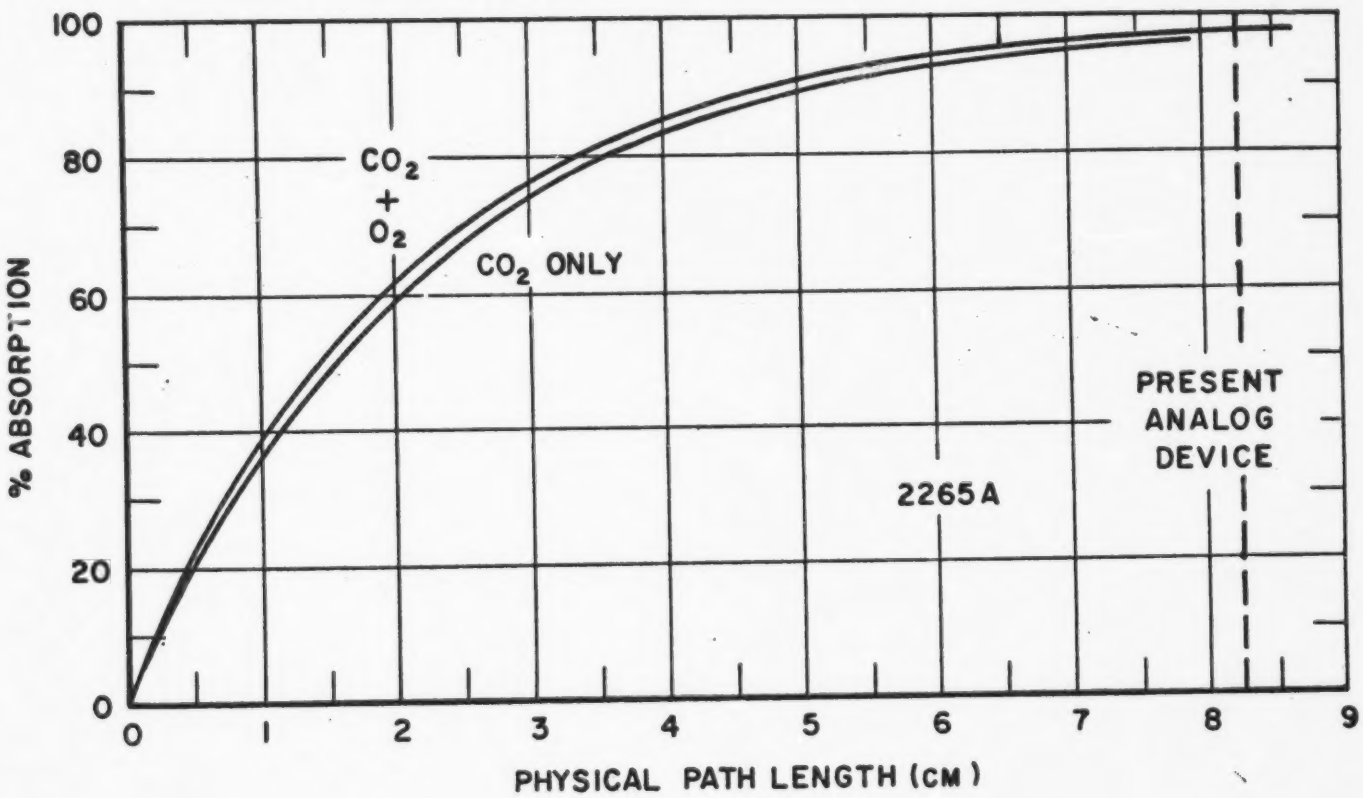

Figure 15 Absorption vs. Pathlength in Products of Constant-Volume Combustion of Stoichiometric Octant/Air

SECTION VII

LIST OF PUBLICATIONS

Hodges, J.L., McAlevy, R.F., III, Potter, J.H., and Kurylko, L., "Nitrogen-Oxide Kinetics in Auto Combustion Products - An Interim Progress Report", Report No. ME-RT-70003, Dept. of Mech. Eng., Stevens Inst. of Tech., Hoboken, N.J., July 1970.

Hodges, J.L., McAlevy, R.F., III, and Potter, J.H., "Nitric-Oxide Generation in a Simulated Spark-Ignition Engine", J. for Eng'g. and Industry (A.S.M.E. Transactions, Series B), Vol. 93, pp. 432-436, 1971.

Hodges, J.L., Kurylko, L., and McAlevy, R.F., III, "Nitric-Oxide Measurements in a Simulated Spark-Ignition Engine", Report No. ME-RT-70008, Dept. of Mech. Eng., Stevens Inst. of Tech., Hoboken, N.J., January 1971.

Preceding page blank

SECTION VIII

REFERENCES

1. Bufalini, J., and Stephens, E., "The Thermal Oxidation of Nitric Oxide in the Presence of Ultraviolet Light", International Journal of Air and Water Pollution, Vol. 9, 1965.

2. Eschenroeder, A., and Martinez, J., "Mathematical Modeling of Photochemical Smog", AIAA Paper, No. 70-116, 1970.

3. Campau, R., and Neerman, J., "Continuous Mass Spectrometic Determination of Nitric Oxide in Automotive Exhaust", SAE Paper No. 660116, 1966.

4. Nicksic, S., and Harkins, J., "Spectrophotometric Determination of Nitric Oxide in Auto Exhaust", Analytical Chemistry, Vol. 34, No. 8, 1962.

5. "Selected Methods for the Measurement of Air Pollutants", U.S. Department of Health, Education, and Welfare PB 169677, 1965.

6. Kaufman, F., and Kelso, J., "Reactions of Atomic Oxygen and Atomic Nitrogen With Oxides of Nitrogen", Seventh Symposium on Combustion, 1959.

7. Wray, K.L., and Teare, J.D., "Shock Tube Study of the Kinetics of Nitric Oxide at High Temperatures", Journal of Chemical Physics, Vol. 36, No. 10, 1962.

8. Wimmer, D., and McReynolds, L., "Nitrogen Oxides and Engine Combustion", SAE Transactions, Vol. 70.

9. Starkman, E., Stewart, H., and Zvonow, V., "An Investigation into the Formation of Emission Precursors", SAE Paper No. 690020, 1969.

10. Newhall, H., "Theoretical and Experimental Investigation of Chemical Kinetics During Rapid Expansion of High Temperature Combustion Products", PhD dissertation, University of California, Berkeley, 1966.

11. LaVoie, F., Heywood, J., and Keck, J., "Experimental and Theoretical Study of Nitric Oxide Formation in Internal Combustion Engines", Combustion Science and Technology, Vol. 1, 1970.

12. Patterson, D., "Cylinder Pressure Variations, A Fundamental Combustion Problem", SAE Paper No. 660129, 1966.

13. Cole, D., and Mirsky, W., "Mixture Motion - Its Effect On Pressure Rise In a Combustion Bomb: A New Look at Cyclic Variation", SAE Paper No. 680766, 1968.

Preceding page blank

14. Peters, B., and Borman, G., "Cyclic Variations and Average Burning Rates in a S.I. Engine", SAE Paper No. 700064, 1970.

15. Herzberg, G., Spectra of Diatomic Molecules, Van Nostrand Co., 2nd ed., 1963.

16. Sullivan, J., and Holland, A., "A Congeries of Absorption Cross Sections for Wavelengths Less Than 3000 Å", NASA CR-371, 1966.

17. Penner, S., Quantitative Molecular Spectroscopy and Gas Emissivities, Addison-Wesley Publishing Co., Boston, Mass., 1959.

18. Brown, W., Gendernalik, S., Kerley, R., and Marsee, F., "Effect of Engine Intake - Air Moisture on Exhaust Emissions", SAE Paper No. 700107, 1970.

19. Spadaccini, L.J., and Chinitz, W., "An Investigation of Nonequilibrium Effects in an Internal Combustion Engine", Journal of Engineering for Power (Transactions of the ASME), April 1972, pp. 98-107.

20. Heywood, J.B., Mathews, S.M., and Owens, B., "Predictions of Nitric Oxide Concentrations in a Spark-Ignition Engine Compared with Exhaust Measurements", Paper No. 710011, presented at the ASE Automotive Engineering Conference, Detroit, Mich., Jan. 11-15, 1971.

21. Cavetto, L.S., Muzio, L.R., Sawyer, R.F., and Starkman, F.S., "The Role of Kinetics in Engine Emission of Nitric Oxide", Combustion Science and Technology, 1971, Vol. 3, pp. 53-61.

22. Muzio, L.J., "Theoretical and Experimental Investigation of Temperature and Composition During Combustion in a Closed System", Doctoral Dissertation, University of California, Berkeley, 1971,(University Microfilm #71-15,849).

23. Hodges, J.L., Kurylko, L., and McAlevy, R.F. III, "Nitric Oxide Measurement in a Simulated Spark Ignition Engine", Report No. ME-RT-73008, Stevens Institute of Technology, Hoboken, N.J., January 31, 1971.

24. Bowman, C.T. and Seery, D.J., "Investigation of NO Formation Kinetics in Combustion Processes: The Methane-Oxygen-Nitrogen Reaction", Paper presented at Symposium on Emissions from Continuous Combustion Systems, General Motors Research Labs., Sept. 27-28, 1971.

25. Generalov, N.A., Losev, S.A., and Maksimenko, V.A., "Absorption of Ultraviolet Radiation By Strongly Heated Carbon Dioxide Gas", Optics and Spectroscopy, Vol. 15, pp. 12-14, 1963.

26. Lavoie, G.A., Heywood, J.B., and Keck, J.C., "Experimental and Theoretical Study of Nitric Oxide Formation in Internal Combustion Engines", Comb. Sci. and Tech., Vol. 1, pp. 313-326, 1970.

27. Shahed, S.M. and Newhall, H.K., "Kinetics of Nitric Oxide Formation in Propane-Air and Hydrogen Air-Diluent Flames", Comb. and Flame, Vol. 17, pp. 131-137, 1971.

28. JANAF Thermochemical Tables, Publication PB 168370, National Bureau of Standards, August 1965.

29. Zeleznik, F.J. and Gordon, S., "A General IBM 704 or 7090 Computer Program for Computation of Chemical Equilibrium Compositions, Rocket Performance, and Chapman-Jouguet Detonations", NASA Technical Note D-1454, October 1962.

30. Bowman, C.T., "Investigation of Nitric Oxide Formation Kinetics In Combustion Processes: The Hydrogen-Oxygen-Nitrogen Reaction", Comb. Sci. and Tech., Vol. 3, pp. 37-45, 1971.

SECTION IX

APPENDIX

Preceding page blank

COMPUTER PROGRAM FOR NITRIC-OXIDE CONCENTRATION CALCULATIONS

Purpose

A FORTRAN IV computer program was written for several purposes:

(1) In its original form [23], the program dealt only with calculations of equilibrium NO concentrations in a constant-volume combustion chamber. The aim of these calculations was to allow comparison with NO concentrations measured post-combustion in the analog device.

(2) The original equilibrium program has been modified slightly for greater precision and flexibility in use and to include kinetic calculation of NO concentrations based on (partial) equilibrium concentrations of other combustion products. The aim of this extension is to allow comparison of theoretical and experimental NO concentrations in the analog device. The basic calculations performed are those for NO concentrations during combustion of hydrocarbon fuels under "normal" conditions representative of automobile-engine combustion after the compression stroke.

(3) As the program was being developed, it appeared that extension of the program to additional capabilities would be desirable. For example, non-hydrocarbon fuels, reactants representing recirculated combustion products, etc. are of current interest. This capability would have allowed broader application of the spark-ignition engine analog device. The abbreviated project scope did not ultimately allow such extension.

Summary of the Program

The program described briefly in this Appendix has the capability for calculating equilibrium product-gas compositions, pressures, and temperatures during and following shell-wise, constant-volume combustion of hydrocarbon fuels from arbitrary initial conditions of equivalence ratio, pressure, and temperature. The chemical species considered are limited to NO, N_2, N, O_2, O, H_2, H, H_2O, OH, CO, and CO_2.

Preceding page blank

In addition to equilibrium calculations and based upon them, kinetic calculations of NO formation are included in the program. In these calculations, a "partial-equilibrium" approach is taken; all species excepting NO are considered to be at equilibrium and NO kinetics are treated via the steady-state approximation for the N atom. Modified Zeldovitch kinetics are considered (Equations (1), (2), and (3); page 7). The OH + N reaction is considered only for the fuel-rich systems.

Provision is also made in the program for outputing the thermodynamic state achieved after homogeneous constant-pressure or constant-volume combustion (of a single "shell") of reactants. This capability was included for its utility in debugging and checking results against published values and with data generated by other programs for more comprehensive thermochemical calculations.

The time scale for kinetic calculations is established via empirical data, specifically via experimental pressure-time histories from the analog device. The program stores and interpolates data for the pressure-time history. The calculated kinetics of NO formation and corresponding equilibrium values for non-NO constituents are linked via the pressure-time history. NO concentrations are calculated at those times when the chamber pressure equals the various chamber pressures calculated to exist after combustion of each individual shell of reactants.

Since the combustion and NO formation are considered to occur stepwise (shell-wise), the equilibrium states of the various shells comprising the total volume and the NO concentration in each are calculated only at discrete times, i.e., at those times corresponding to the end of burning of each shell. At each such time, two NO concentrations are calculated:

(i) the NO concentration calculated (kinetically) assuming NO formation began at the beginning of burning of each shell (overestimate, upper limit)

(ii) the NO concentration calculated (kinetically) assuming NO formation began only upon completion of burning of each shell (underestimate, lower limit).

In each of these cases, the temperatures, pressures and concentrations of non-NO species which are used for calculating the NO concentration are those existing at the end of time period over which NO formation is being calculated.

Figures A-1, A-2, and A-3 diagram the logic of the program. From the figures, it is evident that the equilibrium combustion is treated as a shell-wise constant-pressure combustion followed by isentropic compression of both burned and unburned shells to maintain total chamber volume constant.

Program Inputs

Input values are supplied entirely via FORTRAN IV "DATA" statements in the program (see "Program Listing", below). The following quantities are input:

FORTRAN SYMBOL	
PHI	Equivalence Ratio
P	Initial pressure of reactants
TI	" temperature "
CARB	Carbon atoms per fuel molecule
HYD	Hydrogen " " " "
NS	No. of shells into which chamber is subdivided
NPT	
B1,B2,B3	Coefficients for calculating fuel enthalpy from $H = B1 + B2 \cdot T + B3 \cdot T^2$
C1,C2,C3	Coefficients for calculating fuel entropy from $S = C1 + C2 \cdot \ln T + C3 \cdot T - R \ln P$
MM	Code no. for mode of calculation "0" = only equilibrium results are output "1" = only NO kinetics results are output "2" = both equilibrium and kinetic results are output "3" = only constant-pressure and constant-volume results for burning of single shell are output
PC	Chamber pressures (in atm.) from empirical pressure-time history from analog device scaled to make peak pressure agree with calculated peak pressure.
TE	Times corresponding to chamber pressures from analog device

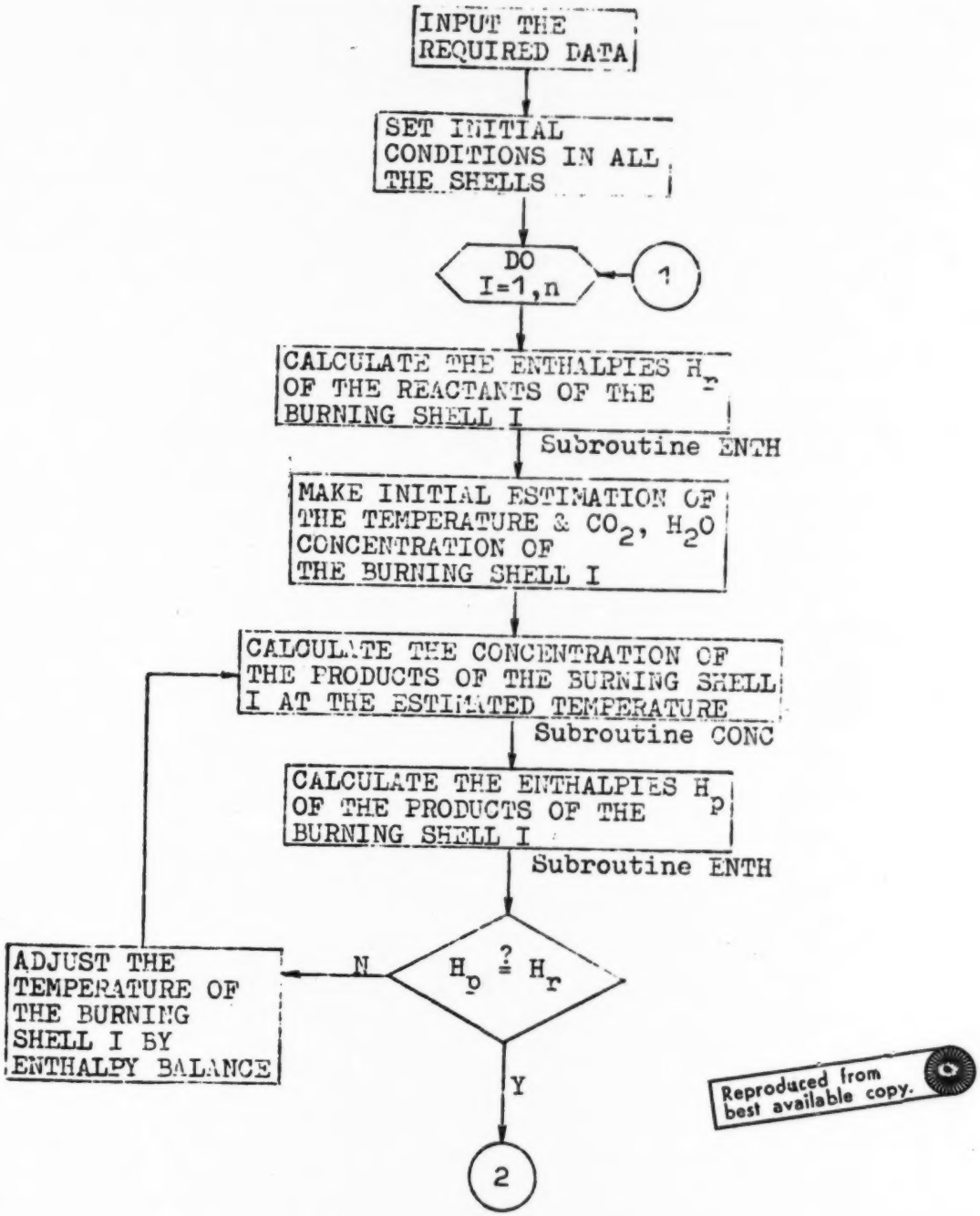
INPUT THE REQUIRED DATA
SET INITIAL CONDITIONS IN ALL THE SHELLS
DO I=1,n
1
CALCULATE THE ENTHALPIES H_r OF THE REACTANTS OF THE BURNING SHELL I
Subroutine ENTH
MAKE INITIAL ESTIMATION OF THE TEMPERATURE & CO_2, H_2O CONCENTRATION OF THE BURNING SHELL I
CALCULATE THE CONCENTRATION OF THE PRODUCTS OF THE BURNING SHELL I AT THE ESTIMATED TEMPERATURE
Subroutine CONC
CALCULATE THE ENTHALPIES H_p OF THE PRODUCTS OF THE BURNING SHELL I
Subroutine ENTH
$H_p \stackrel{?}{=} H_r$
N
ADJUST THE TEMPERATURE OF THE BURNING SHELL I BY ENTHALPY BALANCE
Y
2

Reproduced from best available copy.

Figure A-1 Flow Chart for Equilibrium, Constant-Pressure-Combustion Portion of Program

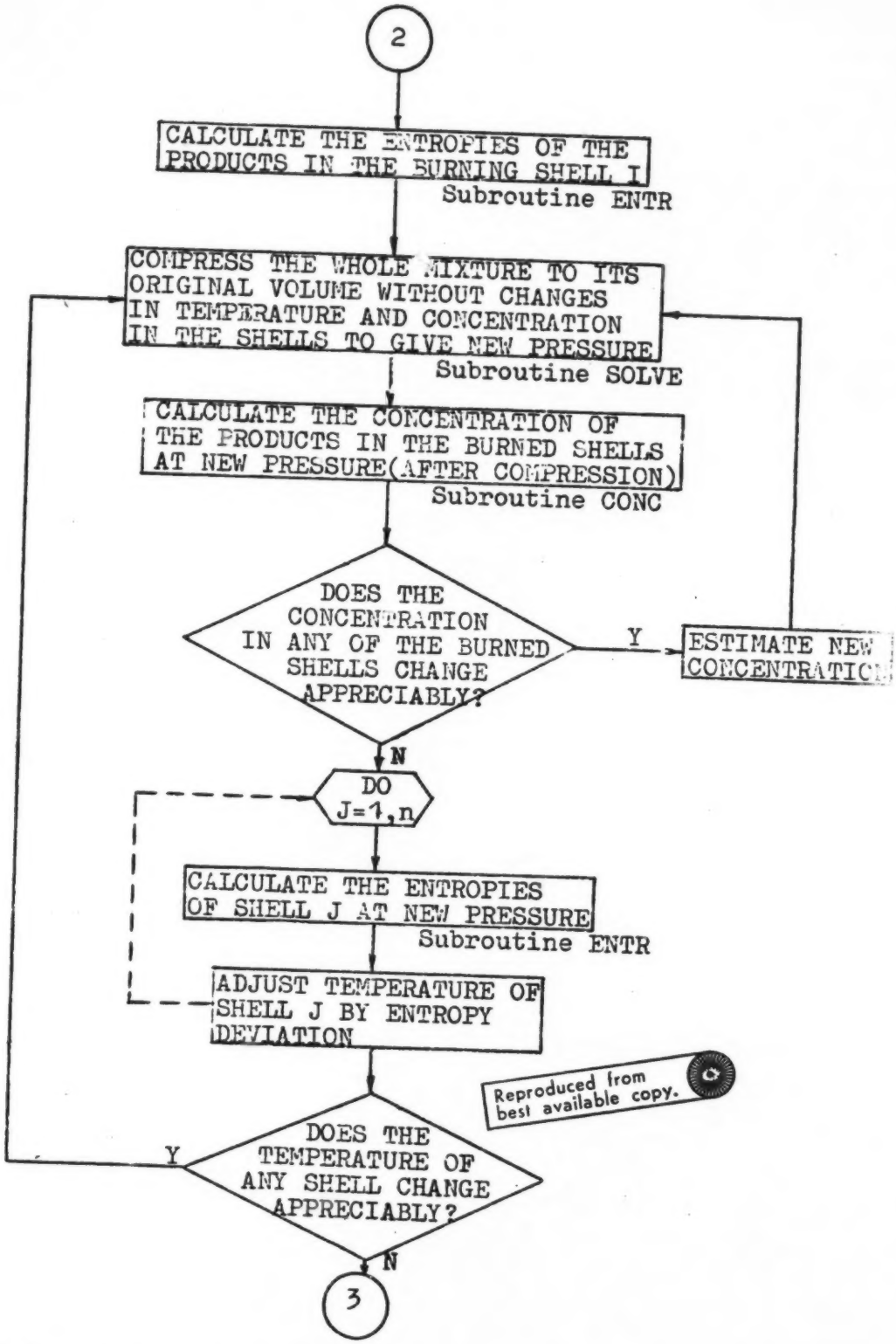
2
CALCULATE THE ENTROPIES OF THE PRODUCTS IN THE BURNING SHELL I
Subroutine ENTR
COMPRESS THE WHOLE MIXTURE TO ITS ORIGINAL VOLUME WITHOUT CHANGES IN TEMPERATURE AND CONCENTRATION IN THE SHELLS TO GIVE NEW PRESSURE
Subroutine SOLVE
CALCULATE THE CONCENTRATION OF THE PRODUCTS IN THE BURNED SHELLS AT NEW PRESSURE(AFTER COMPRESSION)
Subroutine CONC
DOES THE CONCENTRATION IN ANY OF THE BURNED SHELLS CHANGE APPRECIABLY?
Y
ESTIMATE NEW CONCENTRATION
N
DO J=1,n
CALCULATE THE ENTROPIES OF SHELL J AT NEW PRESSURE
Subroutine ENTR
ADJUST TEMPERATURE OF SHELL J BY ENTROPY DEVIATION
Reproduced from best available copy.
DOES THE TEMPERATURE OF ANY SHELL CHANGE APPRECIABLY?
Y
N
3

Figure A-2 Flow Chart for Equilibrium, Isentropic Compression Portion of Program

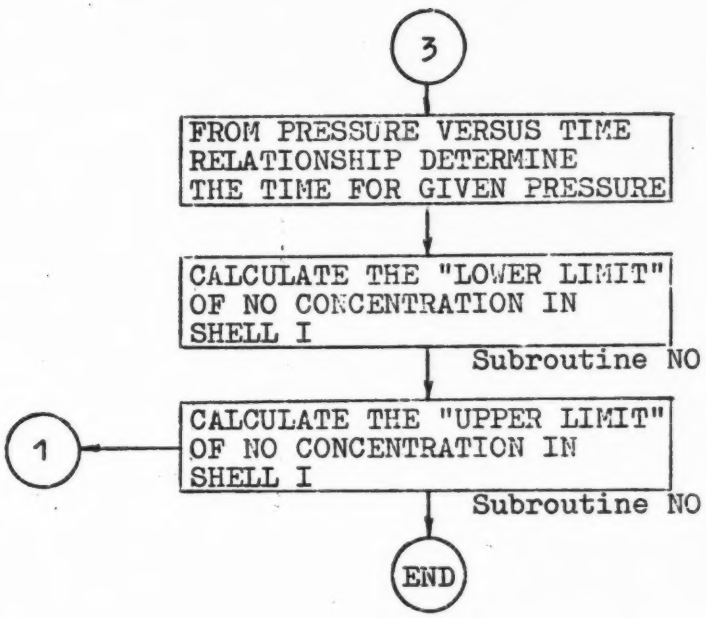
3
FROM PRESSURE VERSUS TIME RELATIONSHIP DETERMINE THE TIME FOR GIVEN PRESSURE
CALCULATE THE "LOWER LIMIT" OF NO CONCENTRATION IN SHELL I
Subroutine NO
1
CALCULATE THE "UPPER LIMIT" OF NO CONCENTRATION IN SHELL I
Subroutine NO
END

Figure A-3 Flow Chart for NO Kinetics Portion of Program

Other specific data included within the program are: (1) the combustion-chamber volume ("VT" of main program) in liters, (2) equilibrium constants ("RK" 's of subroutine "CONC") determined by curve-fitting of tabulated equilibrium-constant data from Ref. 28 (3) coefficients for the temperature dependence of enthalpies (constants of subroutine "ENTH") and of entropies (constants of subroutine "ENTR") drawn from Ref.29, (4) NO reaction-rate constants ("RK" 's of subroutine "NO" from Ref. 30 in conjunction with the corresponding equilibrium constants ("EK" 's of subroutine "NO") from curve-fits of the data of Ref. 28.

Program Output

Figures A-4, A-5, and A-6 show samples of all possible program outputs (Code:"MM" = 2) for a fuel-lean octane/air mixture burning from an initial state at 6.8 atm, 450°K.

Fig. A-4 begins with output showing the format of the equilibrium output data including: (1) the number of the shell being described, (2) its temperature(T) and (3) volume (V), (4) the total no. of moles in that shell (PN) and (5) the numbers of moles of various species (X's). From these results, concentrations (moles/mℓ) or mole fractions are readily calculated depending on the user's interest.

The numerical equilibrium results are then output for all burned shells (1 in Fig. A-4, 2 in Fig. A-5) and for one unburned shell. Since the total chamber volume is subdivided by the program into shells of equal size, the one unburned shell is typical of all unburned shells.

Finally, kinetic results are displayed, including the burning time (after ignition), the pressure, and both the kinetically calculated and the equilibrium NO content of each burned shell. The average NO contents (kinetic and equilibrium) of all burned shells is also output. Each value for NO is in moles. The "overestimated NO" value given is that calculated for the assumption that NO formation in any shell begins when that shell begins to burn.

Figure A-5 shows similar results after completion of burning in two shells out of the total of ten. At this point and for later calculations an "underestimated NO" value is output for all previously burned shells. This value represents the NO formed if it is assumed that each shell begins forming NO when that shell ends burning. Figure A-6 shows an example of the kinetic output (only) after completion of burning by all shells (ten, in this test case).

Figure A-6 is a plot of the kinetic results from the entire output from which Figures A-4 through A-6 are samples.

```
C 8.00 H 18.00  COMBUSTION

EQUIVALENCE RATIO: 0.90
PRESSURE(ATM):   6.804                    TEMPERATURE(K):  450.00


ARRAY OF OUTPUT DATA
P(ATM)
SHELL   T(K)                V(ML)
     PN(J)          X02(J)          XN2(J)          XH2(J)
     XH20(J)        XH1(J)          XOH(J)          X01(J)
     XC02(J)        XC0(J)          XN0(J)



EQUILIBRIUM SCHEME

EQUILIBRIUM STATES AFTER COMBUSTION OF SHELL  1
 10.95
  1  2507.50        0.7782362E-01
     0.4145E-02  0.8054E-04  0.3033E-02  0.6776E-05
     0.5048E-03  0.1310E-05  0.2114E-04  0.2606E-05
     0.4295E-03  0.3521E-04  0.2972E-04
  2   508.49        0.1484215E-01
     0.3898E-02  0.8067E-03  0.3033E-02  0.0000E+00
     0.0000E+00  0.0000E+00  0.0000E+00  0.0000E+00
     0.0000E+00  0.0000E+00  0.0000E+00

KINETIC SCHEME     TIME(MS)=26.0        P(ATM)= 10.95
OVERESTIMATED NO
SHELL     TIME INTERVAL     NO CONCENTRATION    EQUILIBRIUM NO
  1         0.260E+02              0.29E-04             0.30E-04
                        AVERAGE= 0.29E-04  AVERAGE= 0.30E-04
```

Figure A-4 Partial Sample Output from Program - Equilibrium and Kinetic Results After Burning of 1st Shell

```
EQUILIBRIUM SCHEME

EQUILIBRIUM STATES AFTER COMBUSTION OF SHELL  2
 14.91
  1  2636.53       0.6038301E-01
     0.4163E-02  0.8496E-04  0.3033E-02  0.1011E-04
     0.4971E-03  0.2355E-05  0.2882E-04  0.4198E-05
     0.4111E-03  0.5361E-04  0.3770E-04
  2  2482.81       0.5651675E-01
     0.4138E-02  0.7778E-04  0.3033E-02  0.5269E-05
     0.5080E-03  0.8870E-06  0.1801E-04  0.1941E-05
     0.4373E-03  0.2742E-04  0.2798E-04
  3   550.87       0.1181291E-01
     0.3898E-02  0.8067E-03  0.3033E-02  0.0000E+00
     0.0000E+00  0.0000E+00  0.0000E+00  0.0000E+00
     0.0000E+00  0.0000E+00  0.0000E+00

KINETIC SCHEME    TIME(MS)=31.7       P(ATM)= 14.91
UNDERESTIMATED NO(COMPARE WITH LAST OVERESTIMATED NO  CALCULATION)
SHELL    TIME INTERVAL    NO CONCENTRATION    EQUILIBRIUM NO
   1       0.573E+01            0.20E-04            0.30E-04
                    AVERAGE= 0.20E-04  AVERAGE= 0.30E-04
OVERESTIMATED NO
SHELL    TIME INTERVAL    NO CONCENTRATION    EQUILIBRIUM NO
   1       0.574E+01            0.37E-04            0.38E-04
   2       0.573E+01            0.18E-04            0.28E-04
                    AVERAGE= 0.27E-04  AVERAGE= 0.33E-04
```

Figure A-5 Partial Sample Output from Program - Equilibrium and Kinetic Results After Burning of 2nd Shell

KINETIC SCHEME TIME(MS)=54.0 P(ATM)= 44.48

UNDERESTIMATED NO(COMPARE WITH LAST OVERESTIMATED NO CALCULATION)

SHELL	TIME INTERVAL	NO CONCENTRATION	EQUILIBRIUM NO
1	0.194E+00	0.74E-04	0.75E-04
2	0.479E+00	0.58E-04	0.59E-04
3	0.906E+00	0.50E-04	0.50E-04
4	0.150E+01	0.44E-04	0.44E-04
5	0.287E+01	0.39E-04	0.40E-04
6	0.414E+01	0.36E-04	0.36E-04
7	0.558E+01	0.33E-04	0.34E-04
8	0.558E+01	0.30E-04	0.31E-04
9	0.558E+01	0.26E-04	0.29E-04
		AVERAGE= 0.39E-04	AVERAGE= 0.40E-04

OVERESTIMATED NO

SHELL	TIME INTERVAL	NO CONCENTRATION	EQUILIBRIUM NO
1	0.151E+00	0.78E-04	0.79E-04
2	0.363E+00	0.62E-04	0.62E-04
3	0.678E+00	0.53E-04	0.53E-04
4	0.111E+01	0.46E-04	0.47E-04
5	0.168E+01	0.42E-04	0.42E-04
6	0.240E+01	0.38E-04	0.39E-04
7	0.412E+01	0.36E-04	0.36E-04
8	0.558E+01	0.33E-04	0.34E-04
9	0.558E+01	0.31E-04	0.32E-04
10	0.558E+01	0.27E-04	0.30E-04
		AVERAGE= 0.45E-04	AVERAGE= 0.45E-04

Figure A-6 Partial Sample Output from Program - Kinetic Results Only, After Burning of 10th (Last) Shell

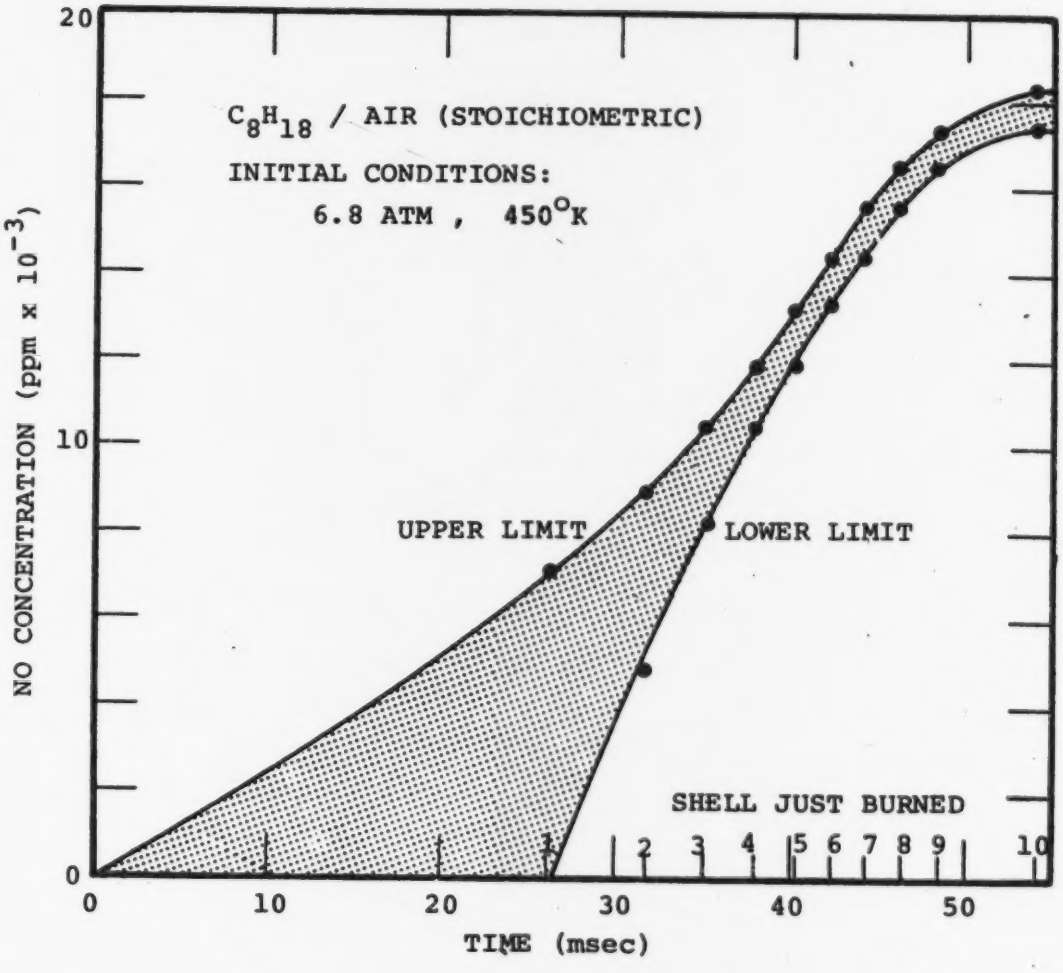

Figure A-7 Calculated Upper and Lower Limits of NO Concentration

Program Checks

Program output was checked, so far as practical, by comparison of results with those from a more comprehensive thermochemical program. The program of Reference 29 (hereafter termed: "reference program") was available for this purpose in the Combustion Laboratory computer-program library. Comparisons were made for two cases.

First, the results of the present program for constant-pressure combustion of a single shell were compared with those from the reference program. This uncovered several shortcomings in the original form of the present program [23], and it was modified accordingly. Results from the two programs agreed very closely.

Second, the calculated total entropy and composition from the present program for constant-volume combustion of a single shell were compared with those calculated by the reference program. Input to the reference program were temperature and pressure after combustion output by the present program. The reference program calculations for composition and total entropy were in excellent agreement with those of the present program.

```
      DIMENSION T(50),V(50),PN(50),FN(50),XO2(50),XN2(50),ENT(50),
     4 PNL(50),ENTN(50),XCO2(50),XCO(50),XH2(50),XH2O(50),XH1(50),
     5 XOH(50),XO1(50),TTN(50),XNO(50),YNO(50),PC(20),TE(20),
     X TF(10),VF(10),XO2F(10),XNOF(10),XO1F(10),XN2F(10),
     X XOHF(10),XH1F(10)
      DATA PHI,P,TI/0.9,6.804,450./
      DATA CARB,HYD/8.,18./
      DATA NS,NPT/10,12/
      DATA B1,B2,B3/-58370.,7.,.03/
      DATA C1,C2,C3/52.89,7.,.06/
      DATA MM/2/
      DATA (PC(LL),LL=1,12)/6.804,7.630,8.354,9.598,12.288,
     1 15.083,20.051,25.434,33.301,40.547,43.858,44.49/
      DATA (TE(LL),LL=1,12)/0.,16.,20.,24.,28.,32.,36.,40.,
     1 44.,48.,52.,54./
      NPT=NPT-1
80    XNUM=CARB+HYD/4.
      PIN=P
      VT=.211403
      WRITE(6,30)CARB,HYD,PHI
30    FORMAT(3H1C F4.2,3H H F5.2,12H  COMBUSTION,/
     X 20HOEQUIVALENCE RATIO: F4.2)
      WRITE(6,31)P,TI
31    FORMAT(16H PRESSURE(ATM): F7.3,10X,17H TEMPERATURE(K): ,F7.2//
      TN=P*VT/(.082*TI)
      FNT=TN*PHI/(PHI+XNUM*4.76)
      RNS=NS
      XCO2(0)=(CARB-.1)*FNT/RNS
      XH2O(0)=(HYD/2.-.1)*FNT/RNS
      XTO2=XNUM/PHI*FNT
      XTN2=3.76*XTO2
      PO2=XTO2/TN*P
      PN2=XTN2/TN*P
      PF=FNT/TN*P
      CALL ENTR(TI,PF,PO2,PH2,PN2,PH1,PO1,PCO2,PCO,PH2O,POH,SF,
     5 SO2,SH2,SN2,SH1,SO1,SCO2,SCO,SH2O,SOH,C1,C2,C3)
      ENTT=FNT*SF+XTN2*SN2+XTO2*SO2
      DO 1 I=1,NS
      T(I)=TI
      V(I)=VT/RNS
      PN(I)=TN/RNS
      FN(I)=FNT/RNS
      XN2(I)=XTN2/RNS
      XO2(I)=XTO2/RNS
      ENT(I)=ENTT/RNS
1     CONTINUE
      IF(MM.EQ.1)GO TO 98
```

Table 2 Program Listing (continued on following pages)

```
      WRITE(6,14)
14    FORMAT(' ARRAY OF OUTPUT DATA'/' P(ATM)'/
     X  ' SHELL',2X,' T(K)',10X,' V(ML)'/5X,' PN(J)',
     X  6X,' XO2(J)',5X,' XN2(J)',5X,' XH2(J)'/5X,
     X  ' XH2O(J)',4X,' XH1(J)',5X,' XOH(J)',5X,' XO1(J)'
     X  /5X,' XCO2(J)',4X,' XCO(J)',5X,' XNO(J)'//)
98    DO 2 I=1,NS
      CALL ENTH(T(I),EF,EO2,EH2,EN2,EH2O,EH1,EOH,EO1,ECO2,
     X  ECO,B1,B2,B3)
      ENF=FN(I)*EF
      ENO2=XO2(I)*EO2
      ENN2=XN2(I)*EN2
      ENTHT=ENF+ENO2+ENN2
      T(I)=T(I)+2000.
      XCO2(I)=XCO2(I-1)
      XH2O(I)=XH2O(I-1)
21    CALL CONC(T(I),P,PHI,PN(I),FN(I),XH2O(I),XH2(I),XH1(I),XOH(I),
     6  XCO2(I),XCO(I),XN2(I),XO2(I),XO1(I),XNO(I),CARB,HYD,XNUM)
      CALL ENTH(T(I),EF,EO2,EH2,EN2,EH2O,EH1,EOH,EO1,ECO2,
     X  ECO,B1,B2,B3)
      ENO2=EO2*XO2(I)
      ENN2=EN2*XN2(I)
      ENH2=EH2*XH2(I)
      ENH2O=EH2O*XH2O(I)
      ENH1=EH1*XH1(I)
      ENCO2=ECO2*XCO2(I)
      ENCO=ECO*XCO(I)
      ENOH=EOH*XOH(I)
      ENO1=EO1*XO1(I)
      ENTHN=ENO2+ENN2+ENH2+ENH2O+ENH1+ENCO2+ENCO+ENOH+ENO1
      TBN=T(I)+(ENTHT-ENTHN)/.16
      IF(ABS(TBN-T(I)).LT..0005*T(I))GO TO 20
      T(I)=(TBN+T(I))/2.
      GO TO 21
20    CONTINUE
      PO2=XO2(I)/PN(I)*P
      PN2=XN2(I)/PN(I)*P
      PH2=XH2(I)/PN(I)*P
      PH2O=XH2O(I)/PN(I)*P
      PH1=XH1(I)/PN(I)*P
      POH=XOH(I)/PN(I)*P
      PO1=XO1(I)/PN(I)*P
      PCO2=XCO2(I)/PN(I)*P
      PCO=XCO(I)/PN(I)*P
      WRITE(6,497)
497   FORMAT(////19H EQUILIBRIUM SCHEME,/)
      IF(MM.EQ.3.AND.I.EQ.1)GO TO 40
      GO TO 51
40    WRITE(6,50)P,I,T(I),PN(I),XO2(I),XN2(I),XH2(I),XH2O(I),
     1  XH1(I),XOH(I),XO1(I),XCO2(I),XCO(I),XNO(I)
50    FORMAT(29H CONSTANT PRESSURE COMBUSTION,/,
     1  1X,F6.2/(1X,I3,2X,F7.2/4X,4E12.4/4X,4E12.4/4X,3E12.4))
51    CALL ENTR(T(I),PF,PO2,PH2,PN2,PH1,PO1,PCO2,PCO,PH2O,POH,SF,
```

```
     5  SO2,SH2,SN2,SH1,SO1,SCO2,SCO,SH2O,SOH,C1,C2,C3)
        SO2=XO2(I)*SO2
        SN2=XN2(I)*SN2
        SH2=XH2(I)*SH2
        SH1=XH1(I)*SH1
        SO1=XO1(I)*SO1
        SCO2=XCO2(I)*SCO2
        SCO=XCO(I)*SCO
        SH2O=XH2O(I)*SH2O
        SOH=XOH(I)*SOH
        ENT(I)=SO2+SN2+SH2+SH1+SO1+SCO2+SCO+SH2O+SOH
  5     CALL SOLVE(VT,NS,P,T,PN,V)
        K=10
        L=10
        DO 3 J=1,I
        PNL(J)=PN(J)
  3     CALL CONC(T(J),P,PHI,PN(J),FN(J),XH2O(J),XH2(J),XH1(J),XOH(J),
     6  XCO2(J),XCO(J),XN2(J),XO2(J),XO1(J),XNO(J),CARB,HYD,XNUM)
        DO 4 J=1,I
        IF(ABS(PN(J)-PNL(J)).LT.1.E-07)GO TO 4
        PN(J)=(PN(J)+PNL(J))/2.
        K=100
  4     CONTINUE
        IF(K.EQ.100)GO TO 5
        DO 6 J=1,NS
        PO2=XO2(J)/PN(J)*P
        PN2=XN2(J)/PN(J)*P
        PH2=XH2(J)/PN(J)*P
        PO1=XO1(J)/PN(J)*P
        PH1=XH1(J)/PN(J)*P
        PCO2=XCO2(J)/PN(J)*P
        PCO=XCO(J)/PN(J)*P
        PH2O=XH2O(J)/PN(J)*P
        POH=XOH(J)/PN(J)*P
        PF=FN(J)/PN(J)*P
        CALL ENTR(T(J),PF,PO2,PH2,PN2,PH1,PO1,PCO2,PCO,PH2O,POH,SF,
     4  SO2,SH2,SN2,SH1,SO1,SCO2,SCO,SH2O,SOH,C1,C2,C3)
        IF(J.GT.I)SF=FN(J)*SF
        SO2=XO2(J)*SO2
        SN2=XN2(J)*SN2
        SH2=XH2(J)*SH2
        SH1=SH1*XH1(J)
        SO1=SO1*XO1(J)
        SCO2=SCO2*XCO2(J,
        SCO=SCO*XCO(J)
        SH2O=SH2O*XH2O(J)
        SOH=SOH*XOH(J)
        IF(J.GT.I)GO TO 7
        ENTN(J)=SO2+SN2+SH2+SH1+SO1+SCO2+SCO+SH2O+SOH
        GO TO 6
  7     ENTN(J)=SN2+SO2+SF
  6     TTN(J)=T(J)*EXP((ENT(J)-ENTN(J))/.19)
```

```
      DO 8 J=1,NS
      IF(ABS(TTN(J)-T(J)).LT..0005*T(J))GO TO 8
      T(J)=(TTN(J)+T(J))/2.
      L=100
8     CONTINUE
      IF(L.EQ.100)GO TO 5
      IF(MM.EQ.1)GO TO 1049
      IF(I.EQ.NS)GO TO 279
      II=I+1
      GO TO 379
279   II=NS
379   WRITE(6,60)I
60    FORMAT(' EQUILIBRIUM STATES AFTER COMBUSTION OF SHELL'I3)
      WRITE(6,70)P,(J,T(J),V(J),PN(J),XO2(J),XN2(J),XH2(J),
     X  XH2O(J),XH1(J),XOH(J),XO1(J),XCO2(J),XCO(J),XNO(J),J=1,II)
70    FORMAT(1X,F6.2/(1X,I3,2X,F7.2,4X,E/4X,4E12.4/4X,
     X  4E12.4/4X,3E12.4))
      IF(MM.EQ.0.OR.MM.EQ.3)GO TO 2
1049  IF(I.EQ.1)TIME=0.0
      TIML=TIME
C     CALCULATE PRESSURE VERSUS TIME
      DO 71 M=1,NPT
      IF(P.GE.PC(M).AND.P.LE.PC(M+1))GO TO 88
      GO TO 71
88    SLOPE=(TE(M+1)-TE(M))/(PC(M+1)-PC(M))
      TIME=TE(M)+(P-PC(M))*SLOPE
      DTIME=TIME-TIML
      WRITE(6,69)TIME,P
69    FORMAT(/15H KINETIC SCHEME,3X,' TIME(MS)=',F4.1,6X,
     2  ' P(ATM)=',F6.2)
      GO TO 72
71    CONTINUE
72    IF(I.EQ.1)GO TO 75
C     NO UNDERESTIMATION
      KODE=1
      WRITE(6,73)
73    FORMAT(' UNDERESTIMATED NO(COMPARE WITH LAST OVERESTIMATED NO
     1  CALCULATION)'/6H SHELL,4X,
     X  13HTIME INTERVAL,4X,16HNO CONCENTRATION,4X,
     X  14HEQUILIBRIUM NO)
      KK=I-1
      SUMF=0.0
      SUMNOF=0.0
      DO 74 J=1,KK
      CALL NO(PHI,KODE,T(J),V(J),YNO(J),XO2(J),XNO(J),XO1(J),
     X  XN2(J),XOH(J),XH1(J),TF(J),VF(J),XO2F(J),XNOF(J),
     X  XO1F(J),XN2F(J),XOHF(J),XH1F(J),TIME,TIML,J,KK,I,DTIME)
      SUMF=SUMF+YNO(J)
      SUMNOF=SUMNOF+XNOF(J)
74    CONTINUE
      RKK=KK
      IF(I.EQ.NS)RKK=RNS
      AVGF=SUMF/RKK
```

Reproduced from best available copy.

```
      AVGNOF=SUMNOF/RKK
      WRITE(6,61)AVGF,AVGNOF
61    FORMAT(21X,' AVERAGE= ',E8.2,11H  AVERAGE= ,E8.2)
C     OVERESTIMATED NO
75    KODE=2
      WRITE(6,76)
76    FORMAT(' OVERESTIMATED NO'/6H SHELL,4X,
     X 13HTIME INTERVAL,4X,16HNO CONCENTRATION,4X,
     X 14HEQUILIBRIUM NO)
      KK=I
      SUMB=0.0
      SUMNOB=0.0
      DO 77 J=1,KK
      CALL NO(PHI,KODE,T(J),V(J),YNO(J),XO2(J),XNO(J),XO1(J),
     X XN2(J),XOH(J),XH1(J),TF(J),VF(J),XO2F(J),XNOF(J),
     X XO1F(J),XN2F(J),XOHF(J),XH1F(J),TIME,TIML,J,KK,I,DTIME)
      SUMB=SUMB+YNO(J)
      SUMNOB=SUMNOB+XNO(J)
77    CONTINUE
      RKK=KK
      AVGB=SUMB/RKK
      AVGNOB=SUMNOB/RKK
      WRITE(6,62)AVGB,AVGNOB
62    FORMAT(21X,' AVERAGE= ',E8.2,11H  AVERAGE= ,E8.2)
      DO 78 J=1,I
      TF(J)=T(J)
      VF(J)=V(J)
      XO2F(J)=XO2(J)
      XNOF(J)=XNO(J)
      XO1F(J)=XO1(J)
      XN2F(J)=XN2(J)
      XOHF(J)=XOH(J)
      XH1F(J)=XH1(J)
78    CONTINUE
2     CONTINUE
      STOP
      END
```

```
      SUBROUTINE CONC(T,P,PHI,PN,FN,H2O,H2,H1,OH,CO2,CO,RN2,O2,O1,
     X  RNO,CARB,HYD,XNUM)
      CDIF=0.0
      ODIF=0.0
      HDIF=0.0
1     PNL=PN
      CON=P/PN
      RK1=10.**(.1321455E05/T-.3061947E01)*SQRT(CON)
      RK2=10.**(-.1087288E04/T+.12194511E01)
      RK3=10.**(.3013006E05/T-.75131088E01)*CON
      RK5=10.**(-.2395742E05/T+.6380064E01)/CON
      RK6=10.**(-.2679026E05/T+.7031926E01)/CON
      RK8=10.**(-.4701074E04/T+.6538625E00)
      O=FN*2.*XNUM/PHI
      C=FN*CARB
      H=FN*HYD
14    IF(PHI.GE.1.0)GO TO 2
303   CO2=C*O2**.5*RK1/(RK2+O2**.5*RK1)
2     H2=(C-CO2)*H2O/(RK2*CO2)
      IF(H2-1.E-07)3,4,4
3     H2=0.00
4     H1=(RK5*(C-CO2)*H2O/(RK2*CO2))**(.5)
      IF(H1-1.E-07)5,6,6
5     H1=0.00
6     OH=(RK2*CO2*H2O/(RK3*(C-CO2)))**(.5)
      IF(OH-1.E-07)7,8,8
7     OH=0.00
C     H ATOM BALANCE
8     HN=2.*H2O+2.*H2+H1+OH
      H2OL=H2O
      H2O=H2O-(HN-H)/2.
      HDIFL=HDIF
      HDIF=H2O-H2OL
      IF(ABS(HDIF).LE.5.E-8)GO TO 9
      IF(HDIFL.EQ..0)GO TO 14
      IF(HDIF/HDIFL)1010,9,14
1010  H2O=(H2O+H2OL)/2.
      GO TO 14
9     OHL=(RK2*CO2*H2O/(RK3*(C-CO2)))**(.5)
      IF(OHL-1.E-07)10,11,11
10    OHL=0.00
11    CO=C-CO2
      IF(CO-1.E-07)12,15,15
12    CO=0.00
15    IF(PHI.LT.1.0)GO TO 17
      O2=(RK2*CO2/(RK1*(C-CO2)))**2
      IF(O2-1.E-07)16,17,17
16    O2=0.00
17    O1=RK6**(.5)*RK2*CO2/(RK1*(C-CO2))
      IF(O1-1.E-07)18,22,22
18    O1=0.00
22    RNO=RK8*(RN2*O2)**.5
      IF(RNO-1.E-07)42,19,19
```

```
 42       RNO=0.00
 C        O ATOM BALANCE
 19       ON=2.*CO2+CO+H2O+OHL+2.*O2+O1+RNO
          IF(PHI.LT.1.0)GO TO 300
          CO2L=CO2
          CO2=CO2-(ON-O)/2.
          CDIFL=CDIF
          CDIF=CO2-CO2L
          IF(ABS(CDIF).LE.5.E-8)GO TO 43
          IF(CDIFL.EQ.0.0)GO TO 14
          IF(CDIF/CDIFL)2010,43,14
 2010     CO2=(CO2+CO2L)/2.
          GO TO 14
 300      O2L=O2
          ODIFL=ODIF
          O2=O2-(ON-O)/2.
          ODIF=O2-O2L
          IF(ABS(ODIF).LE.5.E-8)GO TO 43
          IF(ODIFL.EQ.0.0)GO TO 300
          IF(ODIF/ODIFL)3010,43,303
 3010     O2=(O2+O2L)/2.
          GO TO 303
 43       PN=H2O+H2+H1+OHL+CO2+CO+RN2+O2+O1+RNO
          IF(ABS(PN-PNL)-1.E-07)21,21,1
 21       RETURN
          END
```

```
          SUBROUTINE SOLVE(VT,N,P,T,PN,VS)
          DIMENSION T(50),VS(50),PN(50)
          SUM=0.0
          DO 100 I=1,N
 100      SUM=SUM+PN(I)*.082*T(I)
          P=SUM/VT
          DO 101 I=1,N
 101      VS(I)=PN(I)*.082*T(I)/P
          RETURN
          END
```

```
      SUBROUTINE ENTH(T,EF,E02,EH2,EN2,EH20,EH1,EOH,E01,EC02,
     X  EC0,B1,B2,B3)
      H(T,A,B,C,D,E,F)=1.9869*(A*T+B/2.*T**2+C/3.*T**3+D/4.*T**4+
     6  E/5.*T**5+F)
      IF(T.GT.1000.)GO TO 50
      E02=H(T,3.7189946,-2.5167238E-03,8.5837353E-06,
     8  -8.2998716E-09,2.7082180E-12,-1.0576706E03)
      EN2=H(T,3.6927389,-1.3411998E-03,2.6693385E-06,
     7  -9.9559574E-10,-9.3276676E-14,-1.0629498E03)
      EF=B1+B2*T+B3*T**2
      GO TO 51
50    E02=H(T,3.5980995,7.8056719E-04,-2.2337506E-07,
     8  4.2396622E-11,-3.3419056E-15,-1.1929753E03)
      EN2=H(T,2.8609546,1.5851765E-03,-6.1779901E-07,
     9  1.1119420E-10,-7.5210614E-15,-8.9248972E02)
      EH2=H(T,3.0798700,5.4216636E-04,3.8487619E-08,
     6  -3.4633889E-11,3.6719053E-15,-8.6892051E02)
      EH20=H(T,2.6707532,3.0317115E-03,-8.5351570E-07,
     5  1.1790853E-10,-6.1973568E-15,-2.9888994E04)
      EOH=H(T,2.9029511,9.7345968E-04,-2.0321080E-07,
     8  1.5911612E-11,-5.1673895E-17,3.8779933E03)
      EH1=H(T,2.5026549,-5.2597415E-06,3.3319780E-09,
     4  -8.3272843E-13,7.1462541E-17,2.5471626E04)
      E01=H(T,2.5372567,-1.8422190E-05,-8.8017921E-09,
     7  5.9643621E-12,-5.5743608E-16,2.9230007E04)
      EC02=H(T,4.4008955,3.2163852E-03,-1.3134666E-06,
     9  2.4548216E-10,-1.7094645E-14,-4.8940097E04)
      EC0=H(T,2.9537179,1.5476809E-03,-6.1603844E-07,
     7  1.1272797E-10,-7.7208967E-15,-1.4232807E04)
51    RETURN
      END
```

Reproduced from best available copy.

```
      SUBROUTINE ENTR(T,PF,PO2,PH2,PN2,PH1,PO1,PCO2,PCO,PH2O,
     1 POH,SF,SO2,SH2,SN2,SH1,SO1,SCO2,SCO,SH2O,SOH,C1,C2,C3)
      S(X,Y,A,B,C,D,E,F)=1.9869*(A*ALOG(X)+B*X+C/2.*X**2+D/3.
     2 *X**3+E/4.*X**4+F-ALOG(Y))
      IF(T.GT.1000.)GO TO 200
      SO2=S(T,PO2,3.7189946,-2.5167288E-03,8.5837353E-06,
     4 -8.2998716E-09,2.7082180E-12,3.9080704)
      SN2=S(T,PN2,3.6927389,-1.3411998E-03,2.6693385E-06,
     7 -9.9559574E-10,-9.3276676E-14,2.2827699)
      SF=C1+C2*ALOG(T)+C3*T-1.9869*ALOG(PF)
      GO TO 201
200   SCO2=S(T,PCO2,4.4008955,3.2163852E-03,-1.3134666E-06,
     5 2.4548216E-10,-1.7094645E-14,-6.6437717E-01)
      SCO=S(T,PCO,2.9537179,1.5476809E-03,-6.1603844E-07,
     5 1.1272797E-10,-7.7208967E-15,6.5172790)
      SH2O=S(T,PH2O,2.6707532,3.0317115E-03,-8.5351570E-07,
     5 1.1790853E-10,-6.1973568E-15,6.8838391)
      SH2=S(T,PH2,3.0798700,5.4216636E-04,3.8487619E-08,
     5 -3.4633889E-11,3.6719053E-15,-1.8472212)
      SH1=S(T,PH1,2.5026549,-5.2597415E-06,3.3319780E-09,
     7 -8.3272843E-13,7.1462541E-17,-4.7447219E-01)
      SOH=S(T,POH,2.9029511,9.7345968E-04,-2.0321080E-07,
     7 1.5911612E-11,-5.1673895E-17,5.4854499)
      SO2=S(T,PO2,3.5980995,7.8056719E-04,-2.2337506E-07,
     7 4.2396622E-11,-3.3419056E-15,3.7465771)
      SO1=S(T,PO1,2.5372567,-1.8422190E-05,-8.8017921E-09,
     5 5.9643621E-12,-5.5743608E-16,4.9467942)
      SN2=S(T,PN2,2.8609546,1.5851765E-03,-6.1779901E-07,
     5 1.1119420E-10,-7.5810614E-15,6.3553564)
201   RETURN
      END
```

Reproduced from best available copy.

```
      SUBROUTINE NO(PHI,KODE,T,V,YNO,XO2,XNO,XO1,XN2,XOH,
     X  XH1,TF,VF,XO2F,XNOF,XO1F,XN2F,XOHF,XH1F,TIME,
     X  TIML,J,KK,I,DTIME)
      DIMENSION ZNO(10,2)
      IF(KODE.EQ.1)GO TO 10
      TY=T
      VY=V
      XNOY=XNO
      XO2Y=XO2
      XO1Y=XO1
      XN2Y=XN2
      XOHY=XOH
      XH1Y=XH1
      GO TO 11
10    TY=TF
      VY=VF
      XNOY=XNOF
      XO2Y=XO2F
      XO1Y=XO1F
      XN2Y=XN2F
      XOHY=XOHF
      XH1Y=XH1F
11    VM=1000.*VY
      ZNOE=XNOY/VM
      ZO1=XO1Y/VM
      ZN2=XN2Y/VM
      ZOH=XOHY/VM
      ZO2=XO2Y/VM
      ZH1=XH1Y/VM
      RK1=1.4E14*EXP(-37900./TY)
      RK2=6.4E09*TY*EXP(-3140./TY)
      RK3=4.0E13
      EK1=10.**(-.16480794E05/TY+.6723525)
      EK2=10.**(.7078646E04/TY+.6353725)
      EK3=10.**(.10345546E05/TY-.3851659)
      B=RK1/EK1
      IF(PHI.GE.1.)GO TO 1100
      A=RK2*ZO2
      C=2.*RK1*RK2*ZO1*ZN2*ZO2
      D=2.*RK1*RK2*ZO1/(EK1*EK2)
      GO TO 1150
1100  A=RK2*ZO2+RK3*ZOH
      C=2.*RK1*RK2*ZO1*ZN2*ZO2+2.*RK1*RK3*ZO1*ZN2*ZOH
      D=2.*RK1*RK2*ZO1/(EK1*EK2)+2.*RK1*RK3*ZH1/(EK1*EK3)
1150  IF(J.EQ.KK)GO TO 1200
      ZNOL=ZNO(J,KODE)
```

```
      GO TO 1250
1200  ZNOL=0.0
1250  ZNO(J,KODE)=(ZNOE+ZNOL)/2.
      E=SQRT(C/D)
      H=ALOG(E+ZNOL)
      R=ALOG(E-ZNOL)
1260  F=ALOG(E+ZNO(J,KODE))
      G=ALOG(E-ZNO(J,KODE))
1300  TIMEW=TIML+1000.*(A*(F+R-G-H)/(2.*D*E)-B*(F+G-R-H)/(2.*D))
      IF(ABS(TIME-TIMEW).LE..001*DTIME)GO TO 2111
      IF(ZNO(J,KODE).GE..99*ZNOE.AND.TIMEW.LT.TIME)GO TO 2111
      DER=1000.*(A+E*ZNO(J,KODE))/(D*(E**2-ZNO(J,KODE)**2))
      ZNO(J,KODE)=ZNO(J,KODE)+(TIME-TIMEW)/DER
      IF(ZNO(J,KODE).LT.ZNOE)GO TO 1260
      ZNO(J,KODE)=ZNO(J,KODE)-(TIME-TIMEW)/DER
      ZNO(J,KODE)=(ZNO(J,KODE)+ZNOE)/2.
      GO TO 1260
2111  YNO=ZNO(J,KODE)*VM
      XNOE=ZNOE*VM
      DTIM=TIMEW-TIML
      WRITE(6,4181)J,DTIM,YNO,XNOE
4181  FORMAT(2X,I3,7X,E9.3,12X,E8.2,11X,E8.2)
      RETURN
      END
```

Reproduced from best available copy.